

1 An evolutionarily young defense metabolite influences the root growth of plants via the ancient  
2 TOR signaling pathway.

3

4 Malinovsky F.G.<sup>1</sup>, Thomsen M-L.F.<sup>1</sup>, Nintemann S.J.<sup>1</sup>, Jagd L.M.<sup>1</sup>, Bourguine B.<sup>3</sup>, Burow M.<sup>1</sup>, and  
5 Kliebenstein D. J. <sup>1,2\*</sup>

6

7 <sup>1</sup>DynaMo Center, Copenhagen Plant Science Centre, Department of Plant and Environmental  
8 Sciences, University of Copenhagen, Copenhagen, Denmark

9 <sup>2</sup>Department of Plant Sciences, University of California, Davis, CA, USA

10 <sup>3</sup>Present address: Department of Plant Molecular Biology, University of Lausanne, Switzerland

11 \*Correspondence: Daniel J. Kliebenstein; Email: [kliebenstein@ucdavis.edu](mailto:kliebenstein@ucdavis.edu)

12

### 13 **Abstract:**

14 To optimize fitness a plant should monitor its metabolism to appropriately control growth and  
15 defense. Primary metabolism can be measured by the universally conserved TOR (Target of  
16 Rapamycin) pathway to balance growth and development with the available energy and nutrients.  
17 Recent work suggests that plants may measure defense metabolites to potentially provide a  
18 strategy ensuring fast reallocation of resources to coordinate plant growth and defense. There is  
19 little understanding of mechanisms enabling defense metabolite signaling. To identify mechanisms  
20 of defense metabolite signaling, we used glucosinolates, an important class of plant defense  
21 metabolites. We report novel signaling properties specific to one distinct glucosinolate, 3-  
22 hydroxypropyl glucosinolate across plants and fungi. This defense metabolite, or derived  
23 compounds, reversibly inhibits root growth and development. 3-hydroxypropyl glucosinolate  
24 signaling functions via genes in the ancient TOR pathway. Thus, plants might link evolutionarily  
25 new defense metabolites to ancient signaling pathways to optimize energy allocation.

26

### 27 **Introduction:**

28 Herbivory, pathogen attacks and weather fluctuations are just some of the factors that constantly  
29 fluctuate within a plants environment. To optimize fitness under this wide range of conditions,  
30 plants utilize numerous internal and external signals and associated signaling networks to

31 plastically control metabolism and development (2-4). This metabolic and developmental plasticity  
32 begins at seed germination, where early seedling growth is maintained by heterotrophic  
33 metabolism relying solely on nutrients and energy stored in the seed including the embryo. Upon  
34 reaching light, the seedling transitions to autotrophy by shifting metabolism to initiate  
35 photosynthesis and alters development to maximize photosynthetic capacity (4, 5). Until light is  
36 available, it is vital for the plant to prioritize usage from the maternal energy pool, to ensure the  
37 shoot will breach the soil before resources are depleted. Because the time to obtaining light is  
38 unpredictable, seedlings that had the ability to measure and accordingly adjust their own  
39 metabolism would likely enjoy a selective advantage. In this model, energy availability would be an  
40 essential cue controlling growth throughout a plant's life and not solely at early life-stages. On a  
41 nearly continuous basis, photo-assimilates, such as glucose and sucrose, are monitored and their  
42 internal levels used to determine the growth potential by partitioning just the right amount of  
43 sugars between immediate use and storage (3).

44 Illustrating the key nature of metabolite measurement within plants is that glucose, is  
45 measured by two separate kinase systems that are oppositely repressed and activated to  
46 determine the potential growth capacity, SnRKs1 (sucrose non-fermenting 1 (SNF1)-related  
47 protein kinases 1) and the Target of Rapamycin (TOR) kinase (6). SnRKs1s are evolutionarily  
48 conserved kinases that are activated when sugars are limiting (7). *Arabidopsis thaliana*  
49 (*Arabidopsis*) has two catalytic SnRK1-subunits, KIN10 and KIN11 (SNF kinase homolog 10 and 11),  
50 that activate vast transcriptional responses to repress energy-consuming processes and promote  
51 catabolism (8-10). This leads to enhanced survival during periods of energy starvation. Oppositely,  
52 the TOR kinase is a central developmental regulator, whose sugar-dependent activity controls a  
53 myriad of developmental processes including cell growth, cell-cycle, and cell-wall processes. The  
54 TOR pathway functions to modulate growth and metabolism by altering transcription, translation,  
55 primary and secondary metabolism, as well as autophagy (6, 11). The TOR kinase primarily  
56 functions in meristematic regions where it promotes meristem proliferation. Within these cell  
57 types, TOR measures the sugar content and if the tissue is low in sugar, TOR halts growth, even  
58 overruling hormone signals that would otherwise stimulate growth (12). In plants, TOR functions  
59 within a conserved complex that includes RAPTOR (regulatory-associated protein of TOR) and LST8  
60 (lethal with sec-13 protein 8) (2). RAPTOR likely functions as an essential substrate-recruiting

61 scaffold enabling TOR substrate phosphorylation (4), and LST8 is a seven WD40 repeats protein  
62 with unclear function (13). TOR complex (TORC) activity is positively linked with growth (4) as  
63 mutants in any component lead to qualitative or quantitative defects in growth and development  
64 and even embryo arrest in strong loss-of-function alleles (14, 15). Although the energy sensory  
65 kinases KIN10/11 and TOR sense opposite energy levels, they govern partially overlapping  
66 transcriptional networks, which are intimately connected to glucose-derived energy and  
67 metabolite signaling (6, 10). Having two systems to independently sense sugar shows the  
68 importance of measuring internal metabolism. A key pathway controlled by TOR in all eukaryotes  
69 is autophagy (16, 17). In non-stressed conditions, continuous autophagy allows the removal of  
70 unwanted cell components like damaged, aggregated or misfolded proteins by vacuolar/lysosomal  
71 degradation (18). Under low energy conditions, TORC inhibition leads to an induction of autophagy  
72 to free up energy and building blocks, through degradation of cytosolic macromolecules and  
73 organelles (17). Autophagy-mediated degradation is facilitated by formation of autophagosomes;  
74 double membrane structures that enclose cytoplasmic cargo, and delivers it to the vacuole (17,  
75 19-21).

76 In nature, plant plasticity is not only limited to responding to the internal energy status, but  
77 to an array of external environmental inputs. The multitude of abiotic and biotic factors that  
78 plants continuously face often require choices between contradictory responses, that requires  
79 integrating numerous signals across an array of regulatory levels to create the proper answer. For  
80 example; plant defense against biotic organisms requires coordination of metabolic flux to defense  
81 and development while in continuous interaction with another organisms and the potential for  
82 interaction with other organisms. A proper defense response is vital for the plant as a metabolic  
83 defense response to one organism can impart an ecological cost by making the plant more  
84 sensitive to a different organism (22). Therefore, a plant must choose the most appropriate  
85 defense response for each situation to optimize its fitness and properly coordinate its defense  
86 response with growth and development. A key defense mechanism intricately coordinated across  
87 development is the synthesis of specific bioactive metabolites that are often produced in discrete  
88 tissues at specific times. A current model is that developmental decisions hierarchically regulate  
89 defense metabolism with little to no feed-back from defense metabolism to development.  
90 However, work on the glucosinolate and phenolic pathways is beginning to suggest that defense

91 metabolites can equally modulate development (23-28), thus suggesting that development and  
92 defense metabolism can directly cross-talk.

93

94 To assess if and how defense metabolites can signal developmental changes, we chose to  
95 investigate the glucosinolate (GSL) defense metabolites. The evolution of the core of GSL  
96 biosynthesis is relatively young, and specifically modified GSL structures are even more recent  
97 (29). There are >120 known GSL structures limited to plants from the *Brassicales* order and some  
98 *Euphorbiaceae* family members, with *Arabidopsis* containing at least 40 structures (29). GSLs are  
99 amino acid derived defense metabolites that, after conversion to an array of bioactive  
100 compounds, provide resistance against a broad suite of biotic attackers (29-31). GSLs not only  
101 exhibit a wide structural diversity, but their composition varies depending on environmental  
102 stimuli, developmental stage and even across tissues. This, combined with the information-rich  
103 side chain, makes GSLs not only an adaptable defense system, but also prime candidates for  
104 having distinctive signaling functions. Previous work has suggested that there may be multiple  
105 signaling roles within the GSLs (27, 28, 32-34). Tryptophan-derived indole GSLs or their breakdown  
106 products alter defense responses to non-host pathogens illustrated by biosynthetic mutants  
107 devoid of indole GSLs being unable to deposit PAMP-induced callose in cell walls via an unknown  
108 signal and pathway (32, 34). Similarly, indole GSL activation products have the ability to directly  
109 alter auxin perception by interacting with the TIR1 auxin receptor (23). In contrast to indole GSLs,  
110 mutants in aliphatic GSL accumulation alter flowering time and circadian clock oscillations (35, 36).  
111 The aliphatic GSL activation product, allyl isothiocyanate can induce stomatal closure but it is  
112 unknown if this is specific to allyl GSL or a broader GSL property (33, 37). Allyl GSL (other names  
113 are 2-propenyl GSL and sinigrin) can also alter plant biomass and metabolism in *Arabidopsis* (27,  
114 28). While these studies have provided hints that the GSL may have signaling potential, there is  
115 little understanding of the underlying mechanism or the structural specificity of the signal. To  
116 explore whether built-in signaling properties are a common attribute of GSLs, we screened for  
117 altered plant growth and development in the presence of specific purified aliphatic GSLs. In  
118 particular, we were interested in identifying candidate signals whose activity could ensure fast  
119 repartitioning of resources between development and defense. Here we present a novel signaling  
120 capacity specific to the aliphatic 3-hydroxypropyl glucosinolate (3OHP GSL). Our results suggest

121 that 3OHP GSL signaling involves the universally conserved TOR pathway for growth and  
122 development, as mutants in TORC and autophagy pathways alter responsiveness to 3OHP GSL  
123 application. As such, our findings point towards that evolutionarily young defense metabolites can  
124 signal plastic changes in plant development by interacting with highly conserved signaling  
125 pathways.

126

## 127 **Results:**

### 128 **3OHP GSL inhibits root growth in Arabidopsis**

129 We reasoned that if a GSL can prompt changes in plant growth it is an indication of an inherent  
130 signaling capacity. Using purified compounds, we screened for endogenous signaling properties  
131 among short-chain methionine-derived aliphatic GSLs by testing their ability to induce visual  
132 phenotypic responses in Arabidopsis seedlings. We found that 3OHP GSL causes root meristem  
133 inhibition, at concentrations down to 1 $\mu$ M (Fig. 1A). The observed response is concentration-  
134 dependent (Figure 1A-B). All Arabidopsis accessions accumulate 3OHP GSL in the seeds, and this  
135 pool is maintained at early seedling stages (38-40). Previous research has shown that GSLs in the  
136 seed are primarily deposited in the embryo, accumulating to about 3 $\mu$ mol/g suggesting that we  
137 are working with concentrations within the endogenous physiological range (41, 42).

138

139 We tested how exogenous 3OHP GSL exposure to the roots alters 3OHP GSL accumulation  
140 within the shoot, and how this compares to endogenously synthesized 3OHP GSL levels. We grew  
141 the Col-0 reference accession and the *myb28-1 myb29-1* mutant that is devoid of endogenous  
142 aliphatic GSLs in the presence and absence of exogenous 3OHP GSL. At day 10, the foliar 3OHP GSL  
143 levels were analyzed. Col-0 without treatment had average foliar levels of 3OHP GSL of 3.2  $\mu$ mol/g  
144 and grown on media containing 5 $\mu$ M, 3OHP GSL contributed an additional 2.2  $\mu$ mol/g raising the  
145 total 3OHP GSL to 5.4  $\mu$ mol/g (Figure 1C). The *myb28-1 myb29-1* mutant had no measurable 3OHP  
146 GSL on the control plates and accumulated  $\sim$ 1.4 $\mu$ mol/g upon treatment (Figure 1D). In agreement  
147 with the lower foliar 3OHP GSL accumulation in the *myb28-1 myb29-1* mutant background, this  
148 double mutant had a lower root growth response to exogenous 3OHP GSL (Figure. 1 –figure

149 supplement 1). Importantly, this confirms that the level of 3OHP GSL application is within the  
 150 physiological range.

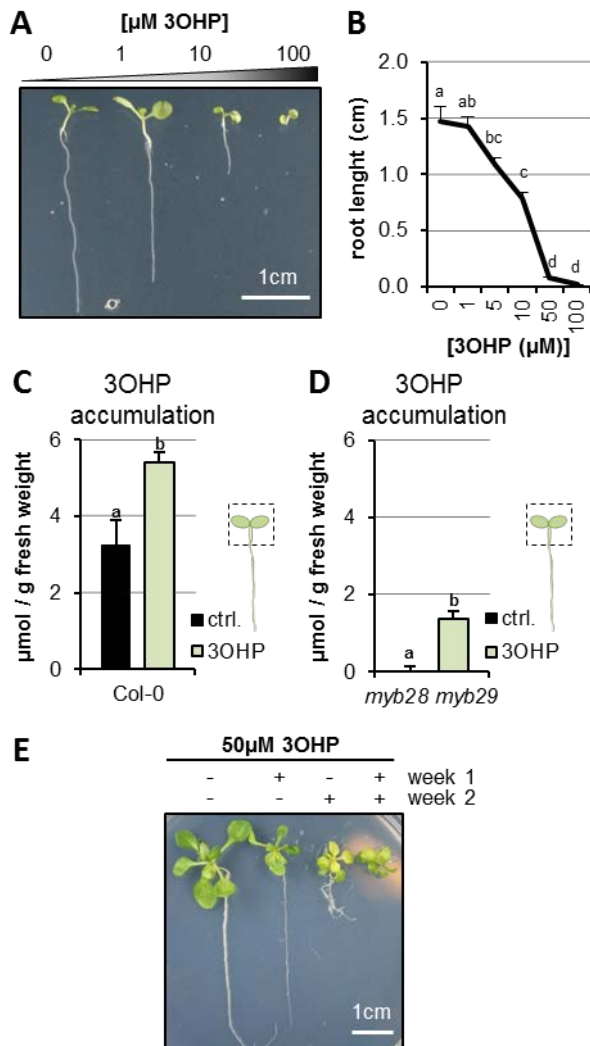


**Figure 1. 3OHP reversibly inhibits root growth.**

**A** 7-d-old seedlings grown on MS medium supplemented with a concentration gradient of 3OHP. **B** Quantification of root lengths of 7-d-old. Results are averages  $\pm$  SE ( $n = 3-7$ ;  $P < 0.001$ ). **C** Accumulation of 3OHP in shoots/areal tissue of 10-d-old Col-0 wildtype seedlings grown on MS medium supplemented with 5μM 3OHP. Results are least squared means  $\pm$  SE over three independent experimental replicates with each experiment having an average eleven replicates of each condition ( $n = 31-33$ ; ANOVA  $P_{\text{Treat}} < 0.001$ ). **D** Accumulation of 3OHP in shoots of 10-d-old *myb28 myb29* seedlings (aliphatic GSL-free) grown on MS medium supplemented with 5μM 3OHP. Results are least squared means  $\pm$  SE over two independent experimental replicates with each experiment having an average of four independent biological replicates of each condition ( $n = 8-14$ ; ANOVA  $P_{\text{Treat}} < 0.001$ ). **E** 14-d-old seedlings grown for 1 week with or without 3OHP as indicated. After one week of development, the plants were moved to the respective conditions showed in week 2.

151

152

153 We then tested if 3OHP GSL or potential activation products inhibit root growth because of  
 154 cell death or toxicity. The first evidence against toxicity came from the observation that even  
 155 during prolonged exposures, up to 14 days of length, Col-0 seedlings continued being vital and  
 156 green (Figure 1E). If there was toxicity the seedlings would be expected to senesce and die. We  
 157 next tested if the strong root growth inhibition by 50μM 3OHP GSL is reversible. Importantly, root  
 158 inhibition is reversible, as the 3OHP GSL-mediated root stunting could be switched on and off by  
 159 transfer between control media and media containing 3OHP GSL (Figure 1E). Based on the toxicity  
 160 and GSL assays, we conclude that the 3OHP GSL treatments are at reasonable levels compared to

161 normal Arabidopsis physiology, and that the phenotypic responses we observed were not caused  
 162 by flooding the system with 3OHP GSL or toxicity.

163

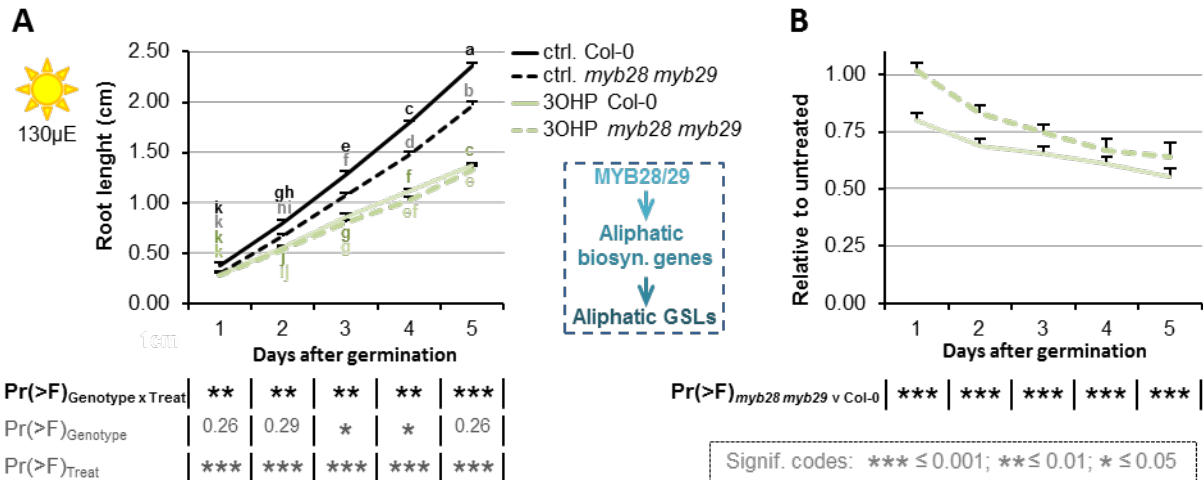


**Figure 1 –figure supplement 1. Root inhibition is affected by endogenous 3OHP/GSLs levels.**

Results are least squared means  $\pm$  SE over three independent experimental replicates with each experiment having an average of ten replicates per condition (n=8-39). **A** Root growth for seedlings grown on MS medium supplemented with or without 5µM 3OHP. Multi-factorial ANOVA was used to test the impact of Genotype (Col-0 v *myb28myb29*), Treatment (Control v 3OHP) and their interaction on root length. The ANOVA results from each day are presented in the table. **B** Root lengths in response to 3OHP (from A) displayed at each time point as relative to the untreated

164

### 165 Root inhibition is specific to 3OHP GSL

166 To evaluate whether 3OHP GSL mediated root inhibition is a general GSL effect or if it is  
 167 structurally specific to 3OHP GSL, we tested if aliphatic GSLs with similar side-chain lengths, but  
 168 different chain modifications, would induce similar root growth effects. First, we assessed 3-  
 169 methylsulfinyl-propyl (3MSP) GSL, the precursor of 3OHP GSL, and the alkenyl-modified three  
 170 carbon glucosinolate allyl (Figure 2A). In contrast to 3OHP GSL, neither of these structurally related  
 171 GSLs possessed similar root-inhibiting activities within the tested concentration range (Figure 2B-  
 172 D). We also analyzed the potential root inhibition for the one carbon longer C4-GSLs 4-  
 173 methylsulfinylbutyl (4MSB) and but-3-enyl (Figure 2E). Neither of these compounds could inhibit  
 174 root growth at the tested concentrations (Figure 2F-H). There is no viable commercial, synthetic or  
 175 natural source for the 4-hydroxybutyl GSL which prevented us from testing this compound. The  
 176 fact that only 3OHP GSL inhibits root elongation suggests that the core GSL structure (comprised  
 177 of a sulfate and thioglucose) does not cause the effect. Importantly, this indicates that 3OHP GSL

178 root inhibition is not a generic result of providing extra sulfur or glucose from the GSL core  
179 structure to the plant, as these compounds would be equally contributed by the other GSLs.  
180 Furthermore, the results confirm that there is no general toxic activity when applying GSLs to

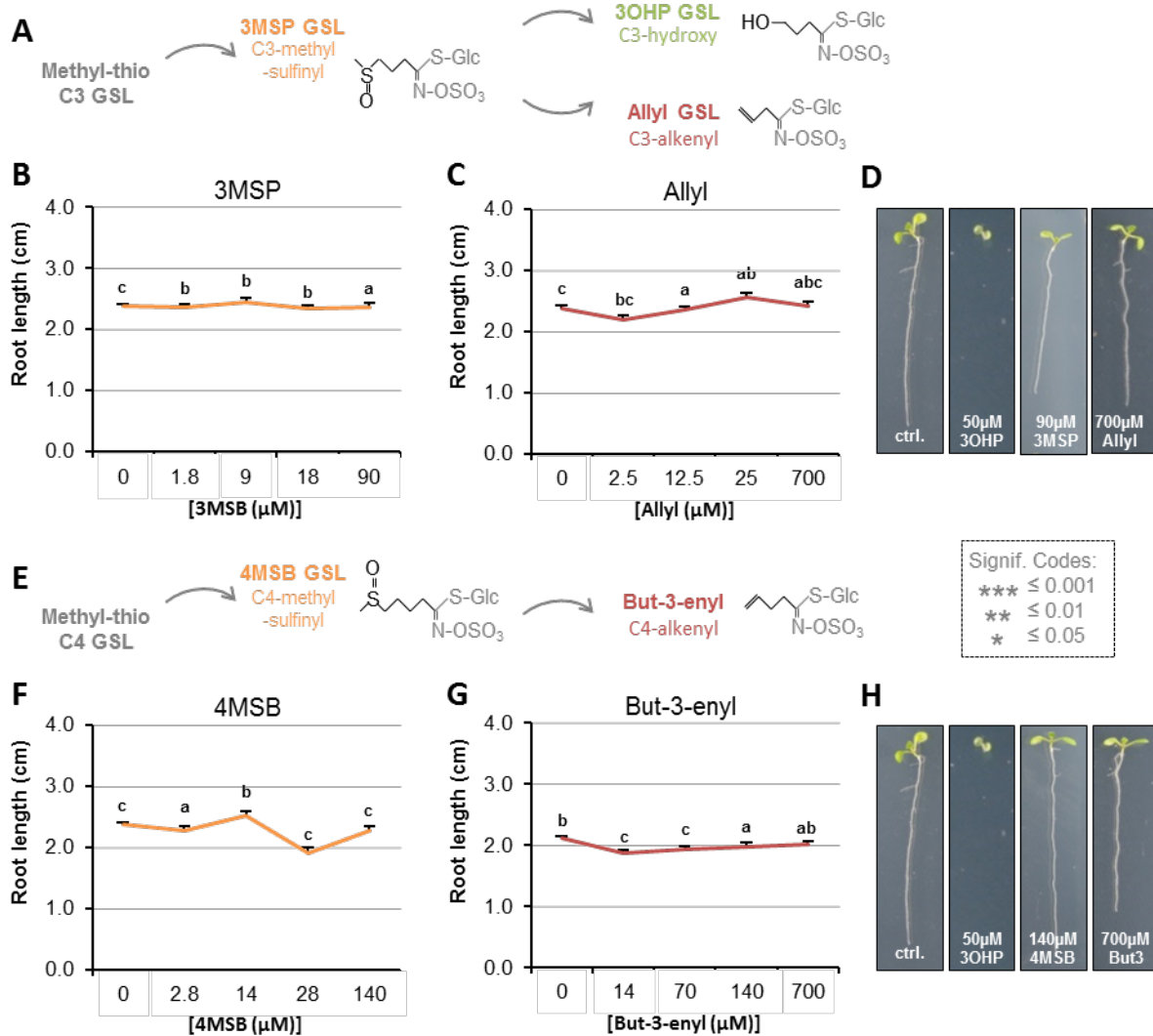


**Figure 2. Root growth is not inhibited by all aliphatic GSLs.**

**A** The aliphatic glucosinolate biosynthetic pathway, from the C3 3-methyl-sulphanyl-propyl (3MSP) to the secondary modified 3-hydroxyl-propyl (3OHP) and 2-propenyl (allyl/sinigrin). **B-C** Root lengths of 7-d-old Col-0 wildtype seedlings grown on MS medium supplemented with a concentration gradient of the indicated aliphatic C3-GSL. The left most point in each plot shows the root length grown in the absence of the specific GSL treatment. Results are least squared means  $\pm$  SE over four independent experimental replicates with each experiment having an average of 21 replicates per condition ( $n_{3MSP}=59-153$ ;  $n_{Allyl}=52-153$ ). Significance was determined via two-way ANOVA combining all experiments. **D** 7-d-old seedlings grown on MS medium with or without 50μM of the indicated GSL. **E** The aliphatic glucosinolate biosynthetic pathway from the C4 4-methyl-sulphanyl-butyl (4MSB) to But-3-enyl. **F-G** Root lengths of 7-d-old Col-0 wildtype seedlings grown on MS medium supplemented with a concentration gradient of the indicated aliphatic C4-GSL. The left most point in each plot shows the root length grown in the absence of the specific GSL treatment. Least squared means  $\pm$  SE over four independent experimental replicates with each experiment having an average of 22 replicates condition ( $n_{4MSB}=38-153$ ;  $n_{But-3-enyl}=68-164$ ). Significance was determined via two-way ANOVA combining all experiments. **H** 7-d-old seedlings grown on MS medium with or without 50μM of the indicated GSL.

182 Arabidopsis. This evidence argues that the 3OHP GSL root inhibition effect links to the specific  
183 3OHP side chain structure, indicating the presence of a specific molecular target mediating the  
184 root inhibition response.

185

### 186 **3OHP GSL responsiveness is wider spread in the plant kingdom than GSL biosynthesis**

187 The evolution of the GSL defense system is a relatively young phylogenetic event that occurred  
188 within the last ~92 Ma and is largely limited to the Brassicales order (43). The aliphatic GSL  
189 pathway is younger still (~60 Ma) and is limited to the Brassicaceae family with the enzyme  
190 required for 3OHP GSL production, AOP3, being limited to *Arabidopsis thaliana* and *Arabidopsis*  
191 *lyrata* within the Arabidopsis lineage (43, 44). However, 3OHP GSL is also found in the vegetative  
192 tissue of the close relative *Olimarabidopsis pumila* (dwarf rocket) (45), and in seeds of more  
193 distant Brassicaceae family members such as the hawkweed-leaved treacle mustard (*Erysimum*  
194 *hieracifolium*), virginia stock (*Malcolmia maritima*), shepherd's cress (*Teesdalia nudicaulis*), and  
195 alpine pennycress (*Thlaspi alpestre*) (46, 47). These species are evolutionarily isolated from each  
196 other, suggesting that they may have independently evolved the ability to make 3OHP GSL (44, 45,  
197 48). As such, 3OHP GSL is an evolutionarily very young compound and we wanted to determine if  
198 the molecular pathway affected by 3OHP GSL is equally young, or whether 3OHP GSL affects an  
199 evolutionarily older, more conserved pathway.

200 First we tested for 3OHP GSL responsiveness in plant species belonging to the GSL-producing  
201 Brassicales order (Figure 3A). We found that 4 of the 5 tested Brassicales species responded to  
202 5 $\mu$ M 3OHP GSL with root growth inhibition regardless of their ability to synthesize 3OHP GSL  
203 (Figure 3B-F). This suggests that responsiveness to 3OHP GSL application does not link to the  
204 ability to make 3OHP GSL. We expanded the survey by including plants within the eudicot lineage  
205 that do not have the biosynthetic capacity to produce any GSLs (Figure 3G) and found that 5 $\mu$ M  
206 3OHP GSL can inhibit root growth in several of the non-Brassicales species tested (Figure 3H-L).  
207 The ability of 3OHP GSL to alter growth extended to *Saccharomyces cerevisiae* where 3OHP GSL led  
208 to slower log phase growth than the untreated control (Figure 3 – Figure Supplement 1). Allyl GSL  
209 in the media had no effect on *S. cerevisiae* growth showing that this was a 3OHP GSL mediated  
210 process (Figure 3 – Figure Supplement 1). The observation that 3OHP GSL responsiveness is  
211 evolutionarily older than the ability to synthesize 3OHP GSL suggests that the molecular target of

212 3OHP GSL, or derived compounds, must be present and highly conserved among these species.  
 213 Similarly, if the signaling event occurs from a 3OHP GSL derivative, then the metabolic processes  
 214 enabling the formation of this derivative are conserved beyond Brassicaceous plants.

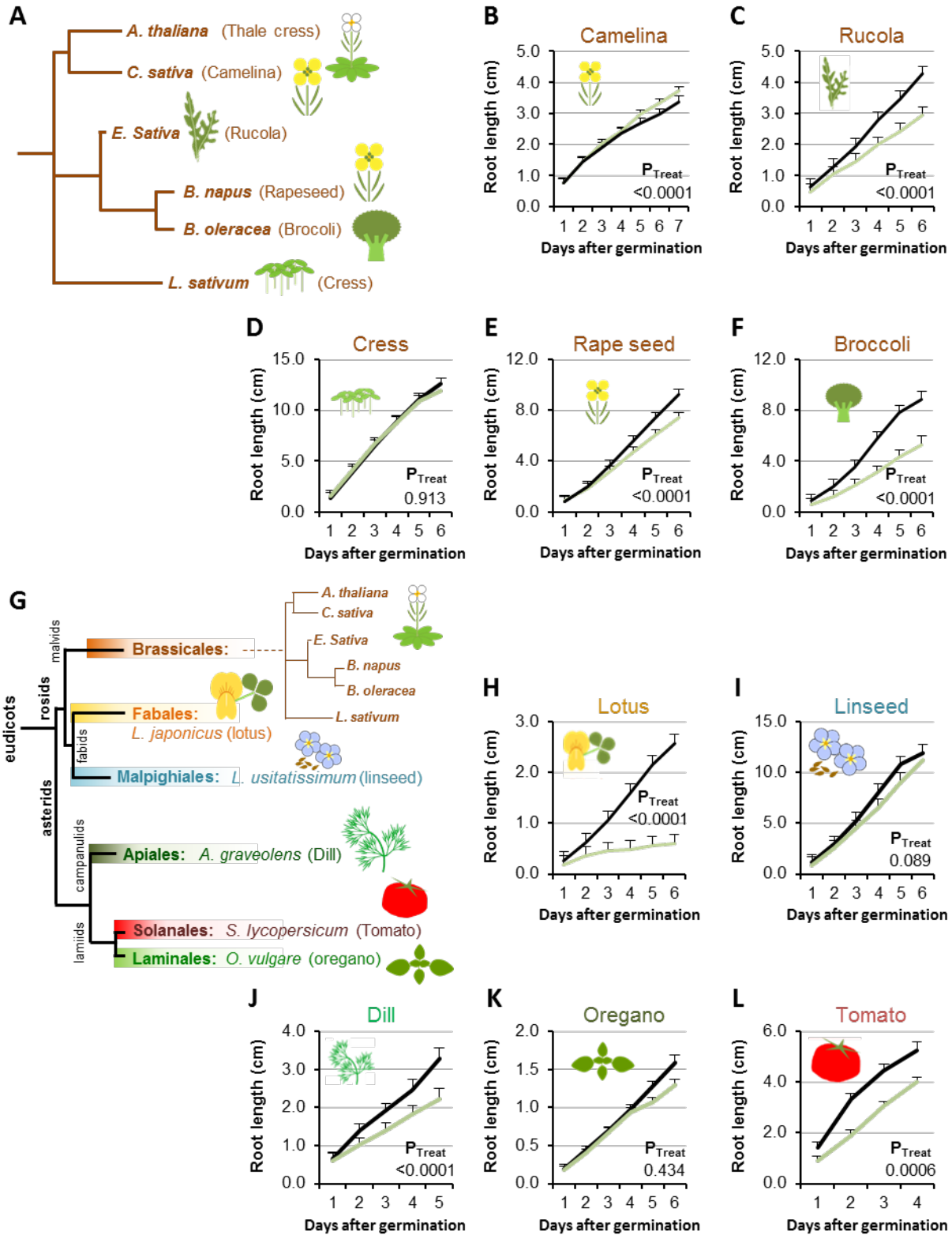


**Figure 3. Conservation of 3OHP responsiveness suggests a evolutionally conserved target.**

**A** Stylized phylogeny showing the phylogenetic relationship of the selected plants from the Brassicales family, branch lengths are not drawn to scale. **B-F** plants from the Brassicales family, grown on MS medium supplemented with or without 5 $\mu$ M 3OHP. **G** Stylized phylogeny showing the phylogenetic relationship of all the selected crop and model plants, branch lengths are not drawn to scale. **H-L** Root growth of plants from diverse eudicot lineages, grown on MS medium supplemented with or without 5 $\mu$ M 3OHP. Results are least squared means  $\pm$  SE for each species using the following number of experiments with the given biological replication. Camelina three independent experimental replicates ( $n_{ctrl}=8$  and  $n_{3OHP}=12$ ). Rucola three independent experimental replicates ( $n_{ctrl}=17$  and  $n_{3OHP}=17$ ). Cress; three independent experimental replicates ( $n_{ctrl}=19$  and  $n_{3OHP}=18$ ). Rape; seed four independent experimental replicates ( $n_{ctrl}=14$  and  $n_{3OHP}=13$ ). Broccoli; three independent experimental replicates ( $n_{ctrl}=10$  and  $n_{3OHP}=13$ ). Lotus; three independent experimental replicates ( $n_{ctrl}=10$  and  $n_{3OHP}=10$ ). Linseed; three independent experimental replicates ( $n_{ctrl}=11$  and  $n_{3OHP}=11$ ). Dill; three independent experimental replicates ( $n_{ctrl}=14$  and  $n_{3OHP}=13$ ). Oregano; four independent experimental replicates ( $n_{ctrl}=40$  and  $n_{3OHP}=39$ ). Tomato; three independent experimental replicates ( $n_{ctrl}=11$  and  $n_{3OHP}=15$ ). A significant effect of treatment on the various species was tested by two-way ANOVA combining all the experimental replicates in a single model with treatment as a fixed effect and experiment as a random effect

215

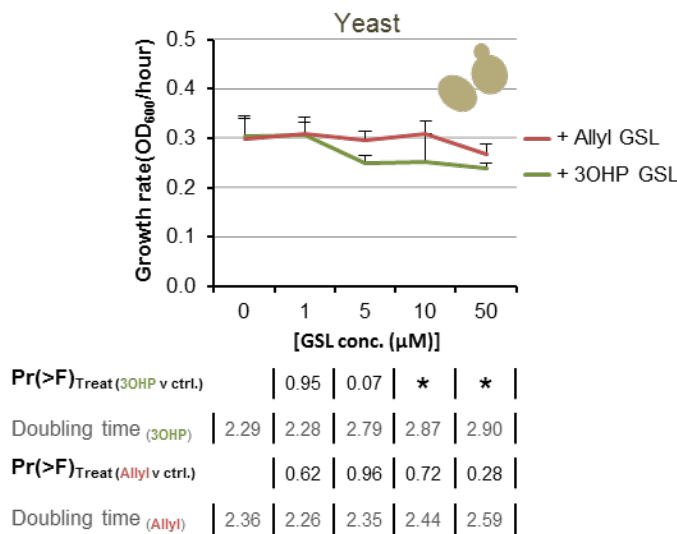


**Figure 3 –figure supplement 1. Yeast response to 3OHP suggests a conserved target throughout eukaryotes.**

Yeast growth in YPD media supplemented with none or increasing levels of 3OHP or Allyl. The hourly OD<sub>600</sub> increase is plotted against each concentration of either Allyl or 3OHP. The least squared means  $\pm$  SE over four replicates are presented (n=4). ANOVA was utilized to test for a significant effect of GLS treatment individually for each concentration of 3OHP and Allyl.

216

**217 3OHP reduces root meristem and elongation zone sizes**

218 We hypothesized that 3OHP GSL application may alter root cellular development to create the  
 219 altered root elongation phenotype. A reduction in root growth can be caused by inadequate cell  
 220 division in the root meristematic zone or by limited cell elongation in the elongation zones (Figure  
 221 4A) (2). To investigate how 3OHP GSL affects the root cellular morphology, we used confocal  
 222 microscopy of 4-d-old Arabidopsis seedlings grown vertically with or without 10 $\mu$ M 3OHP GSL. We

223 used propidium iodide stain to visualize the cell walls of individual cells, manually counted the  
 224 meristematic cells, and measured the distance to the point of first root hair emergence. Root  
 225 meristems of 3OHP GSL treated seedlings were significantly reduced in cell number compared to  
 226 untreated controls (Figure 4B-C). Moreover, we also observed a premature initiation of the  
 227 differentiation zone, as the first root hairs were closer to the root tip upon 3OHP GSL treatment  
 228 (Figure 4 D-E). In addition, we saw bulging and branching of the root hairs in 3OHP GSL treated

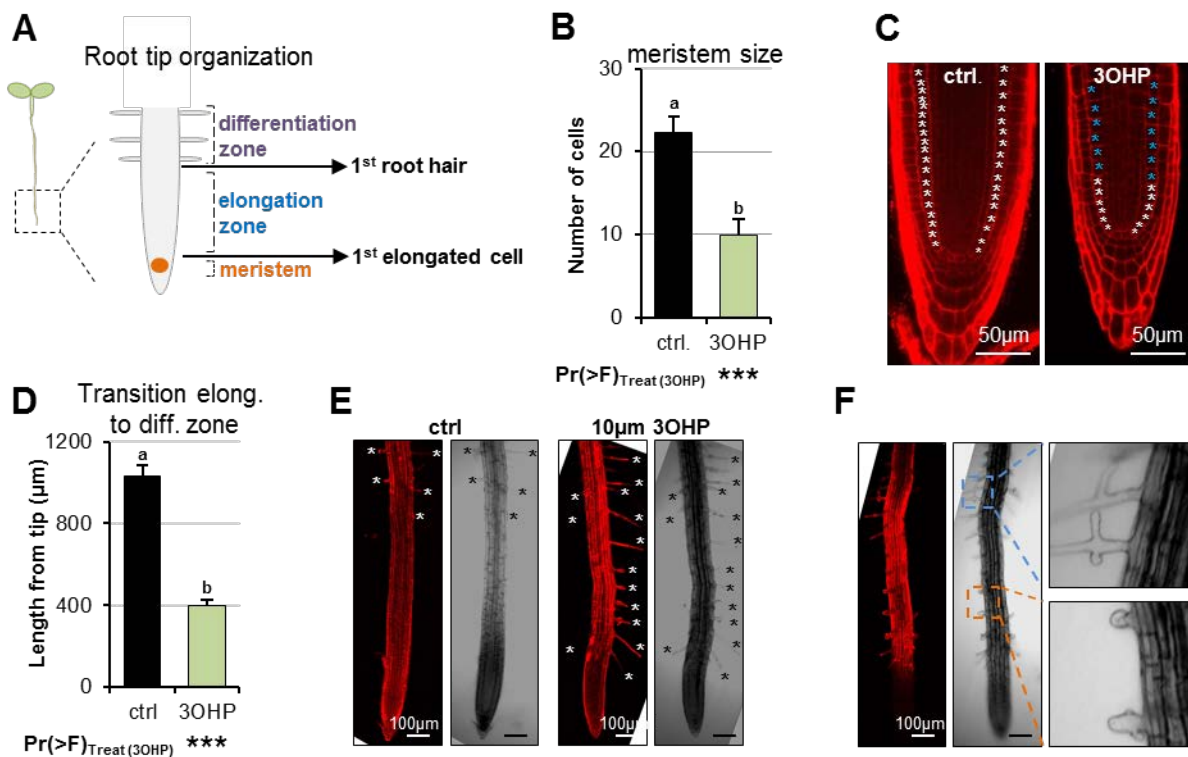


**Figure 4. 3OHP reduces root zone sizes.**

**A** Diagrammatic organization of a root tip; the meristem zone from the QC to the first cell elongation; the elongation zone ends when first root hair appears (1). **B** Meristem size of 4-d-old Arabidopsis seedlings grown on MS medium with sucrose  $\pm$  10µM 3OHP. Results are least squared means  $\pm$  SE over three independent experimental replicates with each experiment having an average of three replicates per condition ( $n_{ctrl}=6$ ;  $n_{3OHP}=9$ ). Significance was tested via two-way ANOVA with treatment as a fixed effect and experiment as a random effect. **C** Confocal images of 4-d-old propidium iodide stained seedlings grown with and without 3OHP. Meristematic cells are marked with white asterisks, elongated cells with blue asterisks. **D** Appearance of first root hair; measured from the root tip on 4-d-old seedlings grown on MS medium with sucrose  $\pm$  10µM 3OHP. Results are least squared means  $\pm$  SE over two independent experimental replicates with each experiment having an average of nine replicates per condition ( $n_{ctrl}=17$ ;  $n_{3OHP}=20$ ). Significance was tested via two-way ANOVA with treatment as a fixed effect and experiment as a random effect. **E** Confocal images of 4-d-old propidium iodide stained seedlings grown with and without 3OHP. Protruding root hairs are marked with white/black asterisks. **F** 3OHP induced root hair deformations, confocal images of 4-d-old propidium iodide stained seedlings grown with 3OHP.

229 roots (Figure 4F). There was no morphological evidence of cell death in any root supporting the  
230 argument that 3OHP GSL is not a toxin. These results indicate that 3OHP GSL leads to root growth  
231 inhibition by reducing the size of the meristematic zone within the developing Arabidopsis root.

232

### 233 **TORC-associated mutants alter 3OHP GSL responsiveness**

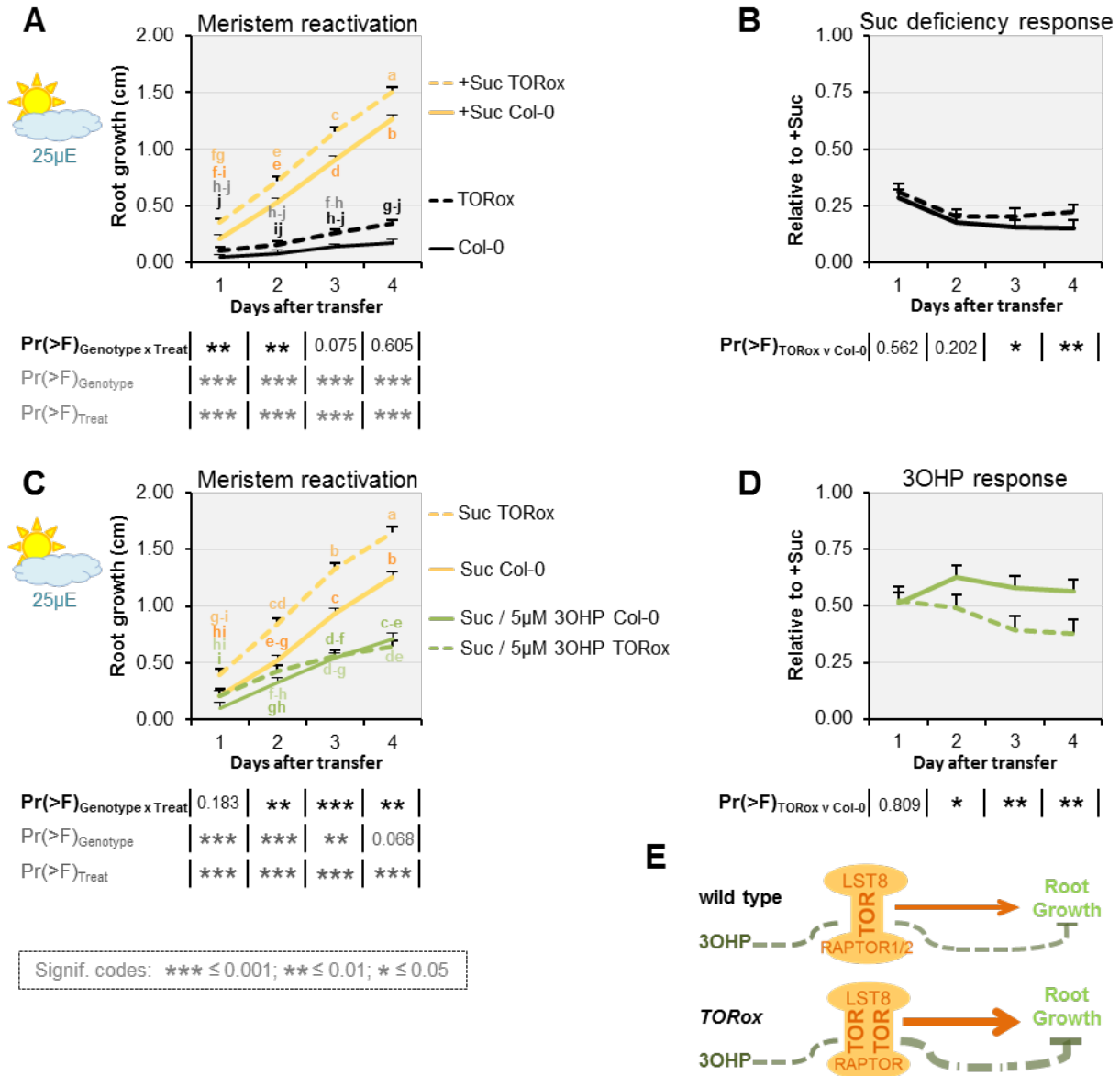
234 The observed response to 3OHP GSL suggests that the target of this compound is evolutionarily  
235 conserved and alters root growth but does not affect the patterning of the root meristem. This  
236 indicates that key root development genes like SHR and SCR are not the targets as they affect  
237 meristem patterning (49, 50). Mutants in GSL biosynthetic genes can lead to auxin over-  
238 production phenotypes as indicated by the superroot (*SUR*) 1 and 2 loci (51, 52). However, the *SUR*  
239 genes are not evolutionarily conserved and 3OHP GSL does not create a superroot phenotype,  
240 showing that the genes are not the targets. A remaining conserved root regulator that does not  
241 alter meristem formation, but still alters root growth, is the TOR pathway (12). Thus, we  
242 proceeded to test if mutants in the TOR pathway alter sensitivity to 3OHP GSL. Because TORC  
243 activity is sugar responsive, we investigated whether 3OHP GSL application may alter the response  
244 to sugar in genotypes with altered TORC activity. We first used the TOR kinase overexpression line  
245 GK548 (TORox) because it was the only one of several published TOR overexpression lines (53)  
246 that behaved as a TOR overexpressor within our conditions (Figure 5 –figure supplement 1). The  
247 GK548 TORox line exhibits accelerated TORC signaling and consequently grows longer roots on  
248 media containing sucrose (Figure 5 and (53)). In addition, GK548 TORox meristems are harder to  
249 arrest (Figure 5B). Applying 3OHP GSL to the GK548 TORox line showed that this genotype had an  
250 elevated 3OHP GSL-mediated inhibition of meristem reactivation in comparison to the WT (Figure  
251 5C-D). This suggests that TORC activity influences the response to 3OHP GSL (Figure 5E).

252

253 We next investigated how genetically disrupting additional components of TORC  
254 affects 3OHP GSL responsiveness. In addition to the catalytic TOR kinase subunit, TORC consists of  
255 the substrate binding RAPTOR (2, 4), and LST8 (13) (Figure 5E). In Arabidopsis- there is one copy of  
256 *TOR*, and two copies of both *RAPTOR* and *LST8* (*RAPTOR1/RAPTOR2* and *LST8-1/LST8-2*) (13, 54).

257

258



259

**Figure 5. TOR over-activation amplifies 3OHP response.**

**A** Root growth for low light grown seedlings. The seedlings were grown on MS medium without sucrose for 3 days, then transferred to the indicated media (Suc; sucrose). Multi-factorial ANOVA was used to test the impact of Genotype (Col-0 v TORox), Treatment (Control v Sucrose) and their interaction on root length. All experiments were combined in the model and experiment treated as a random effect. The ANOVA results from each day are presented in the table. **B** The root lengths grown photo-constrained and without sucrose (from A) displayed at each time point as relative to the respective sucrose activated roots. Results least squared means  $\pm$  SE over three independent experimental replicates with each experiment having an average of nine replicates per condition (n=26-30). Multi-factorial ANOVA was used to test the impact of Genotype (Col-0 v TORox), Treatment (Sucrose v Sucrose/3OHP) and their interaction on root length. All experiments were combined in the model and experiment treated as a random effect. The ANOVA results from each day are presented in the table. **C** Root growth for low light grown seedlings. The seedlings were grown on MS medium without sucrose for 3 days, then transferred to the indicated media. **D** Photo-constrained root lengths in response to sucrose and 3OHP (from A) displayed at each time point as relative to the respective sucrose activated roots. Results are least squared means  $\pm$  SE over two independent experimental replicates with each experiment having an average of six replicates per condition (n=11-14). **E** Schematic model; over

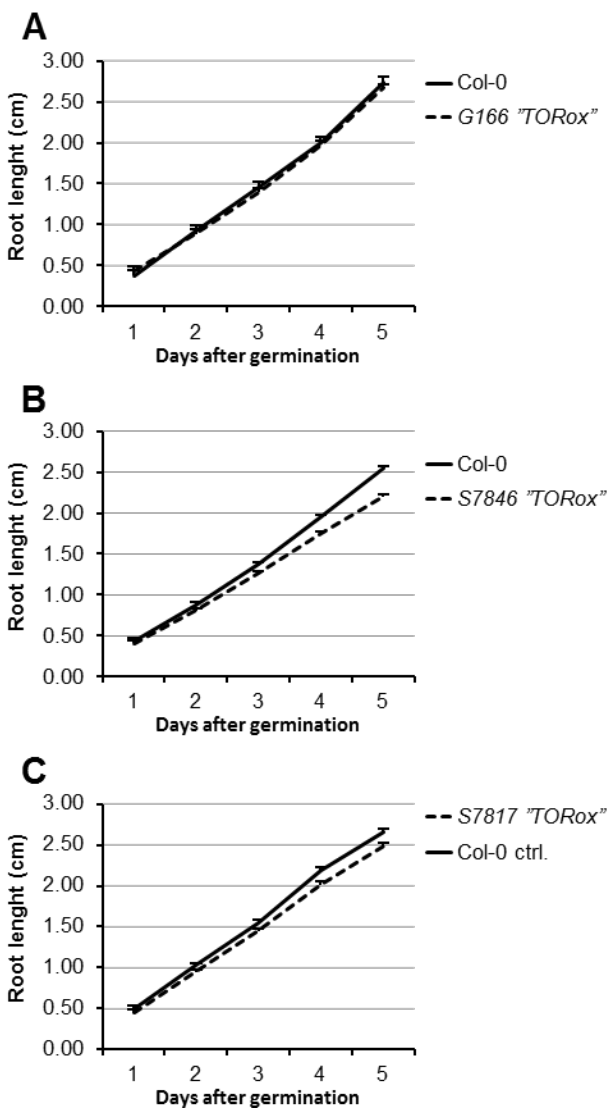


**Figure 5 -figure supplement 1. Published TORox lines that did not display the TORox phenotype under our conditions.**

Multi-factorial ANOVA was used to test the impact of Genotype (Col-0 v specific TORox lines) on root length. All experiments were combined in the model and experiment treated as a random effect. There were no significant differences found. **A** Root growth for the published TORox line G166 and wildtype Col-0 seedlings grown on MS medium supplemented with or without 5 $\mu$ M 3OHP. Results are least squared means  $\pm$  SE (n=8-16). **B** Root growth for the published TORox line S7846 and wildtype Col-0 seedlings grown on MS medium supplemented with or without 5 $\mu$ M 3OHP. Results are least squared means  $\pm$  SE ns across three biological repeats (n=35-45). **C** Root growth for the published TORox line S7817 and wildtype Col-0 seedlings grown on MS medium supplemented with or without 5 $\mu$ M 3OHP. Results are least squared means  $\pm$  SE (n=10-24).

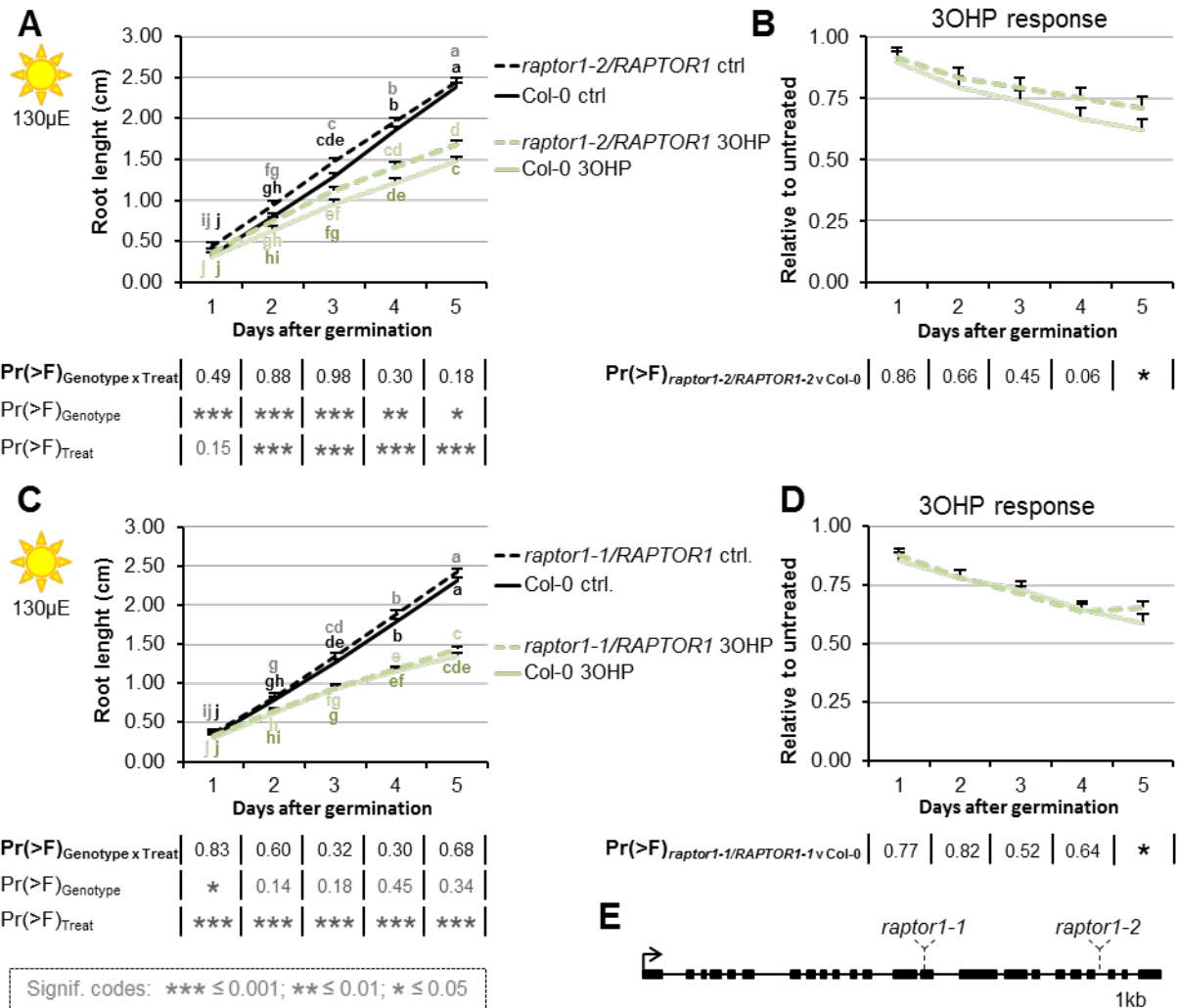


**Figure 5 –figure supplement 2. *RAPTOR1* haplo-insufficiency does not affect 30HP response.**

**A** Root growth for heterozygous *raptor1-2* and wildtype Col-0 seedlings grown on MS medium supplemented with or without 5µM 30HP. Multi-factorial ANOVA was used to test the impact of Genotype (Col-0 v *raptor1-2*), Treatment (Control v 30HP) and their interaction on root length. All experiments were combined in the model and experiment treated as a random effect. The ANOVA results from each day are presented in the table. **B** Root lengths in response to 30HP (from A) displayed at each time point as relative to untreated. Results are least squared means ± SE over three independent experimental replicates with each experiment having an average of six replicates per condition (n=16-19). **C** Root growth for heterozygous *raptor1-1* and wildtype Col-0 seedlings grown on MS medium supplemented with or without 5µM 30HP. Multi-factorial ANOVA was used to test the impact of Genotype (Col-0 v *raptor1-1*), Treatment (Control v 30HP) and their interaction on root length. All experiments were combined in the model and experiment treated as a random effect. The ANOVA results from each day are presented in the table. **D** Root lengths in response to 30HP (from C) displayed at each time point as relative to untreated. Results are least squared means ± SE over three independent experimental replicates with each experiment having an average of seven replicates per condition (n=16-24). **E** Gene structure and T-DNA insertion sites for *RAPTOR1*.

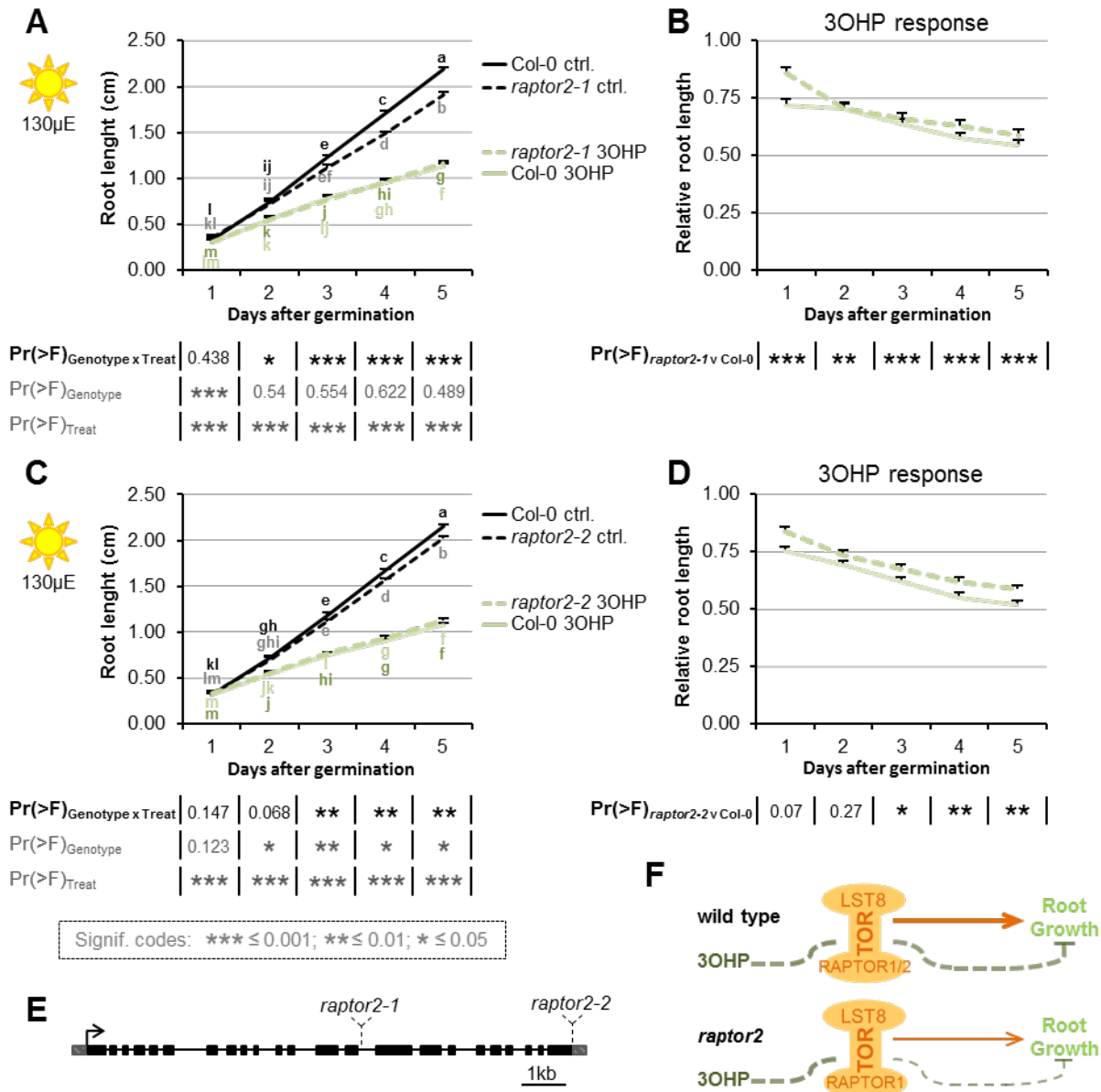


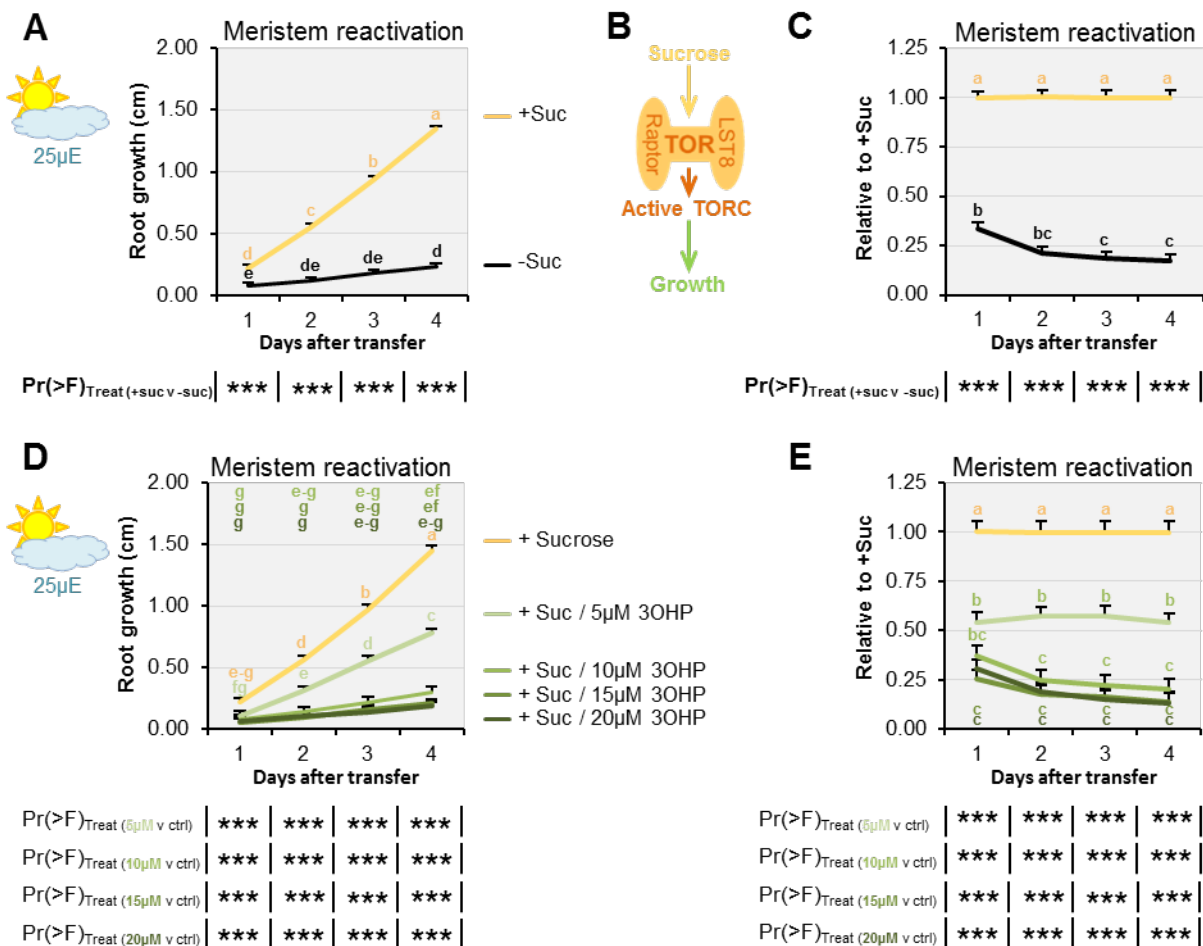
**Figure 5 –figure supplement 3. Loss of one of the two substrate-binding TORC-subunits affect 3OHP response.**

**A** Root growth for *raptor2-1* and wildtype Col-0 seedlings grown on MS medium supplemented with or without 5µM 3OHP. Multi-factorial ANOVA was used to test the impact of Genotype (Col-0 v *raptor2-1*), Treatment (Control v 3OHP) and their interaction on root length. All experiments were combined in the model and experiment treated as a random effect. The ANOVA results from each day are presented in the table. **B** Root lengths in response to 3OHP (from A) displayed at each time point as relative to untreated. Results are least squared means ± SE over four independent experimental replicates with each experiment having an average of thirteen replicates per condition (n=36-68). **C** Root growth for *raptor2-2* and wildtype Col-0 seedlings grown on MS medium supplemented with or without 5µM 3OHP. Multi-factorial ANOVA was used to test the impact of Genotype (Col-0 v *raptor2-1*), Treatment (Control v 3OHP) and their interaction on root length. All experiments were combined in the model and experiment treated as a random effect. The ANOVA results from each day are presented in the table. **D** Root lengths in response to 3OHP (from C) displayed at each time point as relative to untreated. Results are least squared means ± SE over three independent experimental replicates with each experiment having an average of nineteen replicates per condition (n=44-70). **E** Gene structure and T-DNA insertion sites for *RAPTOR2*. **F** Schematic model; loss of one of the substrate-binding subunits *RAPTOR2* decreases growth, and the relative 3OHP response.

263 RAPTOR1 and TOR null mutants are lethal as homozygotes (14, 15), and heterozygous *raptor1*  
 264 mutants did not display a significant change in 3OHP GSL responsiveness (Figure. 5 –figure  
 265 supplement 2). We therefore tested insertion mutants within the weaker homolog *RAPTOR2*,  
 266 whose null mutant is viable, and in our conditions shows mildly reduced root length on sucrose-  
 267 containing media (Figure 5 –figure supplement 3A and C). We found that, for two independent  
 268 insertion lines *raptor2-1* (54, 55) and *raptor2-2* (54) (Figure 5 –figure supplement 3E), there was a  
 269 statistically significant reduction in 3OHP GSL response (Figure 5 –figure supplement 3A-C). This  
 270 supports the hypothesis that 3OHP GSL-associated signaling proceeds through TORC and that  
 271 *RAPTOR2* may play a stronger role in 3OHP perception than *RAPTOR1*.

272

273



Signif. codes: \*\*\* ≤ 0.001; \*\* ≤ 0.01; \* ≤ 0.05

274

275

**Figure 6. 3OHP dampens sugar-mediated meristem activation.**

**A** Root growth for low light grown Col-0 wildtype seedlings. The seedlings were grown on MS medium without sucrose for 3 days, then transferred to the indicated media. Multi-factorial ANOVA was used to test the impact of Treatment on root length. All experiments were combined in the model and experiment treated as a random effect. The ANOVA results from each day are presented in the table. **B** Schematic model; sucrose activates the TOR complex (TORC), leading to growth. **C** The root lengths (from A) displayed at each time point as relative to sucrose activated roots. Results are least squared means  $\pm$  SE over five independent experimental replicates with each experiment having an average of eight replicates per condition ( $n_{-Suc}=43$ ;  $n_{+Suc}=40$ ). **D** Root growth for low light grown seedlings. The seedlings were grown on MS medium without sucrose for 3 days, then transferred to the indicated media. Multi-factorial ANOVA was used to test the impact of Treatment on root length. All experiments were combined in the model and experiment treated as a random effect. The ANOVA results from each day are presented in the table. **E** The root lengths (from D) displayed at each time point as relative to sucrose activated roots (ctrl.). Results are least squared means  $\pm$  SE over two independent experimental replicates with each experiment having an average of seven replicates per condition ( $n=12-16$ ).

276 **3OHP GSL treatment inhibits sugar responses**

277 A key function of TORC activity is to control meristem cell division and this can be measured by  
278 meristem reactivation assays (12). Thus, to further test if TORC dependent responses are altered  
279 by 3OHP GSL, seedlings were germinated in sugar-free media and photosynthesis-constrained  
280 under low light conditions to induce root meristem arrest when the maternal glucose is depleted  
281 (three days after germination). The root meristems were reactivated by applying exogenous  
282 sucrose (Figure 6A-C). By treating arrested root meristems with sucrose alone or in combination  
283 with 3OHP GSL we found that 3OHP GSL could inhibit meristem reactivation of sugar-depleted and  
284 photosynthesis-constrained seedlings (Figure 6D- E). Further, this response was dependent upon  
285 the 3OHP GSL concentration utilized. A similar response was found when treating with a TOR  
286 inhibitor such as rapamycin (12), providing additional support to the hypothesis that 3OHP GSL  
287 may reduce root growth by altering TORC activity.

288  
289 **3OHP GSL pharmacologically interacts with the TOR-inhibitor AZD-8055**

290 To further examine the possibility that 3OHP GSL may be affecting the TOR pathway, we  
291 proceeded to compare the effect of 3OHP GSL to published chemical TOR inhibitors. The active  
292 site TOR inhibitors were originally developed for mammalian cells and inhibit root growth in  
293 various plant species (56). Similar to 3OHP GSL, the active-site TOR inhibitor AZD-8055 (AZD)  
294 induces a reversible concentration-dependent root meristem inhibition (56). By directly comparing  
295 3OHP GSL treatment with known TOR chemical inhibitors in the same system, we can test for

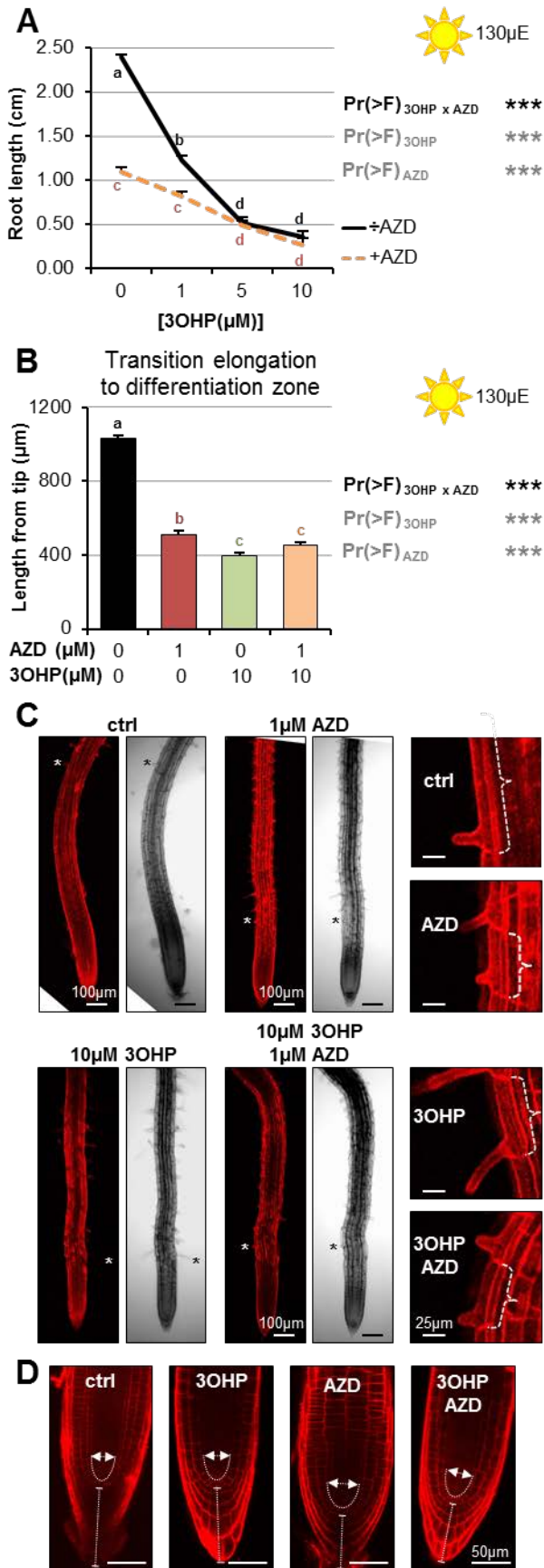


**Figure 7.**

**A** Root lengths of 7-d-old Col-0 wildtype seedlings grown on MS medium with sucrose  $\pm$  combinations of AZD and different concentrations of 3OHP. Results are least squared means  $\pm$  SE over three independent experimental replicates with each experiment having an average of nine replicates per condition (n=18-58). Multi-factorial ANOVA was used to test the impact of the two treatments and their interaction on root length. All experiments were combined in the model and experiment treated as a random effect. The ANOVA results from each day are presented in the table. **B** Appearance of first root hair; measured from the root tip on 4-d-old seedlings grown on the indicated MS medium with sucrose. Results are least squared means  $\pm$  SE over two independent experimental replicates with each experiment having an average of nine replicates per condition (n=17-20). Multi-factorial ANOVA was used to test the impact of the two treatments and their interaction on root length. All experiments were combined in the model and experiment treated as a random effect. The ANOVA results from each day are presented in the table. **C** Confocal images of 4-d-old propidium iodide stained seedlings. The first protruding root hairs are marked with white/black asterisks on the left panel. Right panel shows zooms of first root hair, cell size is indicated. **D** Confocal images of 4-d-old propidium iodide stained seedlings.

297 interactions between 3OHP GSL and the known TOR inhibitors. An interaction between 3OHP GSL  
 298 application and a known TOR inhibitor, e.g. an antagonistic relationship, is an indication that the  
 299 same target is affected. To assess whether interactions between 3OHP GSL and TOR signaling

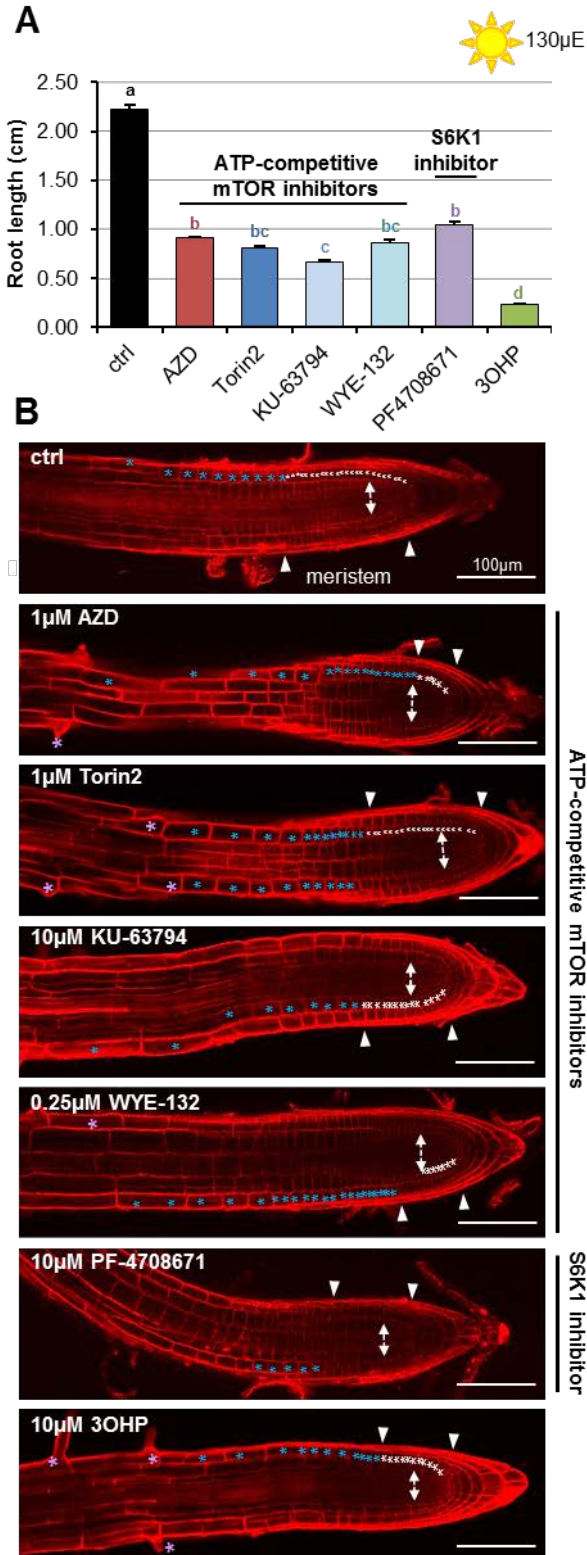


**Figure 7 –figure supplement 1.**

**A.** Root lengths of 7-d-old Col-0 wildtype seedlings grown on MS medium with sucrose ± the indicated mTOR or S6K inhibitors. Results are averages ± SE (n=8-41). **B** Confocal images of 4-d-old propidium iodide stained seedlings. Meristematic cells are marked with white asterisks, elongated cells with blue, and cells belonging to the differentiation zone are marked with purple asterisks. Arrows indicate approximate meristem sizes.

300 occur, we grew seedlings vertically on media with combinations of 3OHP GSL and AZD and root-  
301 phenotyped the plants to compare the effect on root morphology. This identified a significant  
302 antagonistic interaction between AZD and 3OHP GSL (3OHP x AZD), both in terms of root length  
303 response (Figure 7A) and in initiation of the differentiation zone (Figure 7B). This antagonistic  
304 interaction is also supported by the appearance of first root hair (Figure 7B), as the premature  
305 initiation of the differentiation zone in the presence of 10  $\mu$ M 3OHP GSL did not change further  
306 upon co-treatment (Figure 7B). Moreover, there was a vast overlap in the phenotypic response to  
307 both compounds (Figure 7C-D); notably the closer initiation of the root differentiation zone to the  
308 root tip (Figure 7B-C) and the decreased cell elongation (Figure 7C, right panel). Together, this  
309 suggests that the TOR inhibitor AZD and 3OHP GSL have a target in the same signaling pathway as  
310 no additive effect is observed. Supporting this is the observation that 3OHP GSL treatment is  
311 phenotypically similar to a range of TOR active site inhibitors, as well as an inhibitor of S6K1 (one  
312 of the direct targets of TOR) (Figure 7 –figure supplement 1).

313 Interestingly, the short root hair phenotype induced by AZD showed a synergistic  
314 interaction between AZD and 3OHP GSL suggesting that they may target different components of  
315 the TORC pathway that interact (Figure 7C). Further, while there is strong phenotypic overlap  
316 between AZD and 3OHP GSL, there are also specific activities. AZD induced a rounding of the root  
317 tip (1), but co-treatment with 3OHP GSL restored a wildtype-like tip phenotype (Figure 7D). The  
318 lack of root rounding and root hair inhibition suggest that AZD and 3OHP GSL both target the TOR  
319 pathway, but at different positions. Alternatively, the 3OHP GSL may be a more specific TOR  
320 inhibitor and the additional AZD phenotypes could be caused by the ATP-competitive inhibitor  
321 having alternative targets in plants. Together, these results suggest that 3OHP GSL directly or  
322 indirectly targets the same molecular pathway as known TOR inhibitors (57).

323

### 324 **Blocking parts of the autophagy machinery affects 3OHP GSL associated signaling**

325 Activation or repression of the TOR pathway leads to regulatory shifts in numerous downstream  
326 pathways (Figure 8E) (6, 11). For example, active TOR negatively regulates autophagy across  
327 eukaryotic species including Arabidopsis (16, 17). To test if pathways downstream of TORC are  
328 affected by, or involved in, 3OHP GSL signaling, we analyzed mutants of two key autophagic (ATG)

329 components, *atg2-1* (18) and *atg5-1* (58). ATG2 is part of the ATG9 cycling system that is essential  
 330 for autophagosome formation (19, 59, 60). ATG9-containing vesicles are a suggested membrane  
 331 source for the autophagosome, and vesicles containing ATG9 are cycled to-and-from the  
 332 phagophore via the ATG9 cycling system (19, 60). ATG5, is part of the dual ubiquitin-like  
 333 conjugation systems responsible for ATG8 lipidation (19, 60, 61). There are nine *ATG8* paralogues  
 334 in Arabidopsis (60) and together with the single copy of *ATG5*, they are essential for  
 335 autophagosome initiation, expansion, closure, and vacuolar fusion (19, 60). After the first

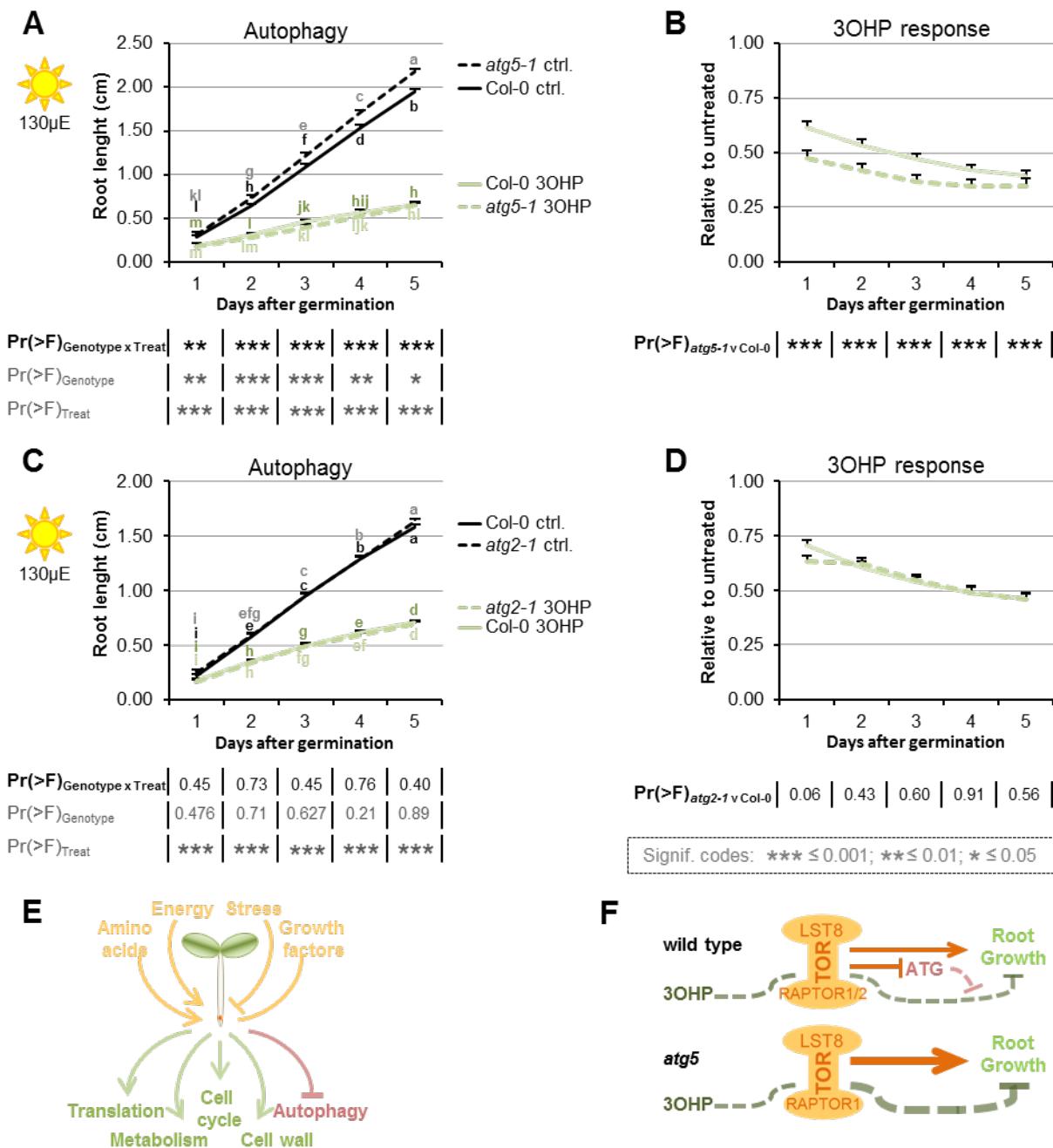


**Figure 8. Blocking autophagosome elongation amplifies the 3OHP response.**

**A** Root growth for *atg5-1* and wildtype Col-0 seedlings grown on MS medium supplemented with or without 5 $\mu$ M 3OHP. Multi-factorial ANOVA was used to test the impact of Genotype (Col-0 v *atg5-1*), Treatment (Control v 3OHP) and their interaction on root length. All experiments were combined in the model and experiment treated as a random effect. The ANOVA results from each day are presented in the table. **B** Root lengths in response to 3OHP (from A) displayed at each time point as relative to untreated. Results are least squared means  $\pm$  SE over two independent experimental replicates with each experiment having an average of 21 replicates per condition (n=31-52). **C** Root growth for *atg2-1* and wildtype Col-0 seedlings grown on MS medium supplemented with or without 5 $\mu$ M 3OHP. Multi-factorial ANOVA was used to test the impact of Genotype (Col-0 v *atg2-1*), Treatment (Control v 3OHP) and their interaction on root length. All experiments were combined in the model and experiment treated as a random effect. The ANOVA results from each day are presented in the table. **D** Root lengths in response to 3OHP treatment (from C) displayed at each time point as relative to untreated. Results are least squared means  $\pm$  SE over two independent experimental replicates with each experiment having an average of 26 replicates per condition (n=36-66). **E** The TOR complex (TORC), is affected by several upstream input, leading to activation or repression of several downstream pathways. **F** Schematic model; sucrose activates TORC, leading to root growth. 3OHP represses root growth through interaction with TORC. Autophagy pathways via ATG5 negatively affect 3OHP response.

336  
337 conjugation system has conjugated ATG8 to an E2-like enzyme, the E3 ligase-like activity of the  
338 second ATG5-containing system enables ATG8 lipidation at the autophagic membrane (19, 62, 63).  
339 We found that *atg5-1* enhanced 3OHP GSL responsiveness (Figure 8A-B) while *atg2-1* had a wild  
340 type response (Figure 8C-D). One possible explanation for this difference between the two  
341 mutants is that, apart from macro-autophagy, plants also have micro-autophagy (60), a process  
342 that, in animal systems, has been shown to be negatively regulated by TOR (64). Micro-autophagy  
343 does not involve *de novo* assembly of autophagosomes, and ATG5 has been shown to be involved  
344 in several forms of micro-autophagy whereas the role of ATG2 is more elusive and may not be  
345 required (64). Thus, the elevated 3OHP GSL response in the *atg5-1* mutant supports the  
346 hypothesis that 3OHP GSL signaling proceeds through the TOR pathway, but also suggests that this  
347 response requires parts of the autophagic machinery as it was not observed for *atg2-1*.

348

349 **Discussion**

350 In this study we describe a novel signaling capacity associated with 3OHP GSL, a defense  
351 metabolite present in the Brassicaceae Arabidopsis, and provide evidence that the linked signal  
352 proceeds via the TOR pathway. Application of exogenous 3OHP GSL caused reversible root  
353 meristem inhibition by morphological reprogramming of the root zones, i.e. dramatically reduced  
354 the root meristem size and limited root cell elongation (Figure 4). This response occurred at levels  
355 within the endogenous range and there was no evidence of cell death in any treated root,

356 suggesting that this is not a toxicity response (Figure 1). Additionally, these morphological  
357 responses were specific to 3OHP GSL and not caused by any structurally or biosynthetically related  
358 GSL, suggesting that these responses were not because of generic properties shared by GSLs  
359 (Figure 2). Exposing a wide phylogenetic array of plants, including lineages that have never  
360 produced GSLs, to 3OHP GSL showed that application of this compound can inhibit growth broadly  
361 across the plant kingdom as well as in yeast (Figure 3, Figure 3 –figure supplement 1). This  
362 suggests conservation of the downstream signaling pathway across these diverse plant lineages.  
363 Equally, if the signaling compound is not 3OHP GSL itself, but a derivative, then the required  
364 biosynthetic processes must be conserved. This conservation largely rules out the specific GSL  
365 activation pathway controlled by Brassicales specific thioglucosidases, myrosinases (65-67). The  
366 phylogenetic conservation of the 3OHP GSL response led us to search for a target pathway  
367 controlling growth and development that would be evolutionary well conserved between the  
368 tested species.

369

370 By comparing the root phenotype identified with 3OHP GSL application to the published  
371 literature, we hypothesized that 3OHP GSL treatment may affect TORC, a key primary metabolic  
372 sensor that controls growth and development, and is conserved back to the last common  
373 eukaryotic ancestor (2). Active site TOR inhibitors inhibit root growth in numerous plant species  
374 similar to 3OHP GSL application (56), supporting the hypothesis that 3OHP GSL may function via  
375 TORC. A model with 3OHP GSL affecting TORC would explain how 3OHP GSL can alter root  
376 development across the plant kingdom (Figure 3). Mechanistic support for this hypothesis came  
377 from a number of avenues. First, 3OHP GSL can block the TOR-mediated sugar activation of  
378 arrested meristems (Figure 6). Second, the TORox mutant intensifies 3OHP GSL linked signaling  
379 (Figure 5), and correspondingly loss-of-function mutants of the substrate binding TORC  
380 component *raptor2* diminish the 3OHP GSL effect (Figure 5 –figure supplement 3). Additionally,  
381 there are clear phenotypic overlaps between the root phenotypes induced by known TOR  
382 inhibitors and 3OHP GSL, e.g. root inhibition, inhibition of cell elongation, and notably the  
383 dramatic reduction of the meristem sizes (Figure 7). Critically, 3OHP GSL and known TOR inhibitors  
384 were antagonistic for a number of phenotypes. In pharmacology, the outcomes of a drug  
385 combination can either be antagonistic, additive or synergistic, depending on whether the effect is

386 less than, equal to, or greater than the sum of the effects of the two drugs (57). Antagonistic  
387 interactions, as observed with 3OHP GSL and AZD, can occur if two drugs exhibit mutual  
388 interference against the same target site, or if their targets converge on the same regulatory hub  
389 (57). Together, these lines of evidence suggest that 3OHP GSL targets the TOR pathway to alter  
390 root meristem development within Arabidopsis and potentially other plant species.

391         Extending the analysis to pathways downstream of TORC, showed that loss of ATG5, a vital  
392 component of the autophagic machinery (16, 17), intensifies the 3OHP GSL response (Figure 8A-  
393 DB). This supports the hypothesis that 3OHP GSL signaling proceeds through the TOR complex, but  
394 also suggest that this signal requires parts of the autophagic machinery. Loss of another  
395 autophagic component, ATG2, did not influence the 3OHP response (Figure 8C-D). Together, this  
396 raises the possibility that 3OHP GSL responses involve predominantly a micro-autophagy pathway,  
397 which is ATG5- but may not be ATG2-dependent, rather than the macro-autophagy pathway that  
398 depends upon both genes (60) (64). Micro-autophagy removes captured cytoplasmic components  
399 directly at the site of the vacuole via tonoplast invagination. The cargo to be degraded ranges from  
400 non-selective fractions of the cytoplasm to entire organelles, dependent on the type of micro-  
401 autophagy. The two ubiquitin-like conjugation systems, and thereby ATG5, have been shown to be  
402 involved in several forms of micro-autophagy, such as starvation-induced, non-selective, and  
403 glucose-induced selective autophagy (64). Interestingly, micro-autophagy involves vacuolar  
404 movement of cargo, and the vacuole is considered the main storage site for glucosinolates [51].  
405 Thus, ATG5 may be responsible for enabling the movement of exogenously applied 3OHP GSL out  
406 of the cytoplasm where it could interact with the TORC pathway and into the vacuole. This would  
407 decrease the concentration of the 3OHP GSL signal and could explain why the *atg5-1* mutant is  
408 more sensitive to 3OHP GSL. Further work is required to test if ATG5 is functioning to attenuate  
409 the 3OHP GSL signal.

410         A conundrum for defense signaling compounds to affect growth is the evolutionary age  
411 discrepancy; defense metabolites are typically evolutionarily very young, as they are often species  
412 or taxa specific, while growth regulatory pathways are highly conserved across broad sets of plant  
413 taxa. This raises the question of which mechanism(s) may allow this connection between young  
414 metabolites and old regulatory pathways. This suggests that plants may sense young metabolites

415 using evolutionarily old signaling pathways. Similar evidence is coming from other secondary  
416 metabolite systems suggesting that this may be a general phenomenon. For example, an indolic  
417 GSL activation product can interact with the conserved *TIR1* auxin receptor to alter auxin  
418 sensitivity within *Arabidopsis* (23). Similarly, an unknown phenolic metabolite appears to affect  
419 regulation of growth and development by influencing the Mediator complex that is conserved  
420 across all eukaryotes (24-26); and the plant polyphenol resveratrol directly inhibits the mammalian  
421 TOR to induce autophagy (68). Thus, young plant metabolites can influence evolutionarily  
422 conserved pathways. Interestingly, this strongly resembles the action of virulence-associated  
423 metabolites within plant pathogens. Pseudomonad bacteria produce the evolutionarily young  
424 coronatine that alters the plant defense response by interacting with the conserved JA-Ile receptor  
425 *COI1* (69). In plant/pathogen interactions, this ability of pathogen-derived metabolites to alter  
426 plant defense signaling is evolutionarily beneficial because it boosts the pathogens virulence *in*  
427 *planta*. It is less clear if this selective pressure model also applies to plant defense compounds that  
428 interact with endogenous signaling pathways. Following the plant/pathogen derived model, such  
429 plant defense metabolites might have been co-selected on the ability to affect the biotic attacker  
430 and simultaneously provide information to the plant. However, these examples may simply be  
431 serendipitous cases, where the defense metabolite happened to interact with a pathway. Testing  
432 these hypotheses would require a broad survey to assess how many plant metabolites can affect  
433 signaling within the plant. This survey would also be required to assess how frequently defense  
434 metabolites may play signaling roles within plants and what the targeted pathways are.

435

436 Within this report, we provided evidence that 3OHP GSL, or derived compounds, appears  
437 to function as a natural endogenous TORC inhibitor that can work across plant lineages. This  
438 creates a link whereby the plant's endogenous defense metabolism can simultaneously coordinate  
439 with growth. Such a built-in signaling capacity would allow coordination between development  
440 and defense, as the plant could use the defense compound itself as a measure of the local  
441 progress of any defense response and readjust development and defense to optimize against the  
442 preeminent threat. Future work is required to identify the specific molecular interaction that  
443 allows this communication to occur, this will help to illuminate how and why plants measure their  
444 own defense metabolism to coordinate available resources more broadly with growth. Future

445 work might also ascertain whether there is a broader class of plant produced TOR inhibitors. If this  
446 is true, they might be highly useful in understanding TOR function across kingdoms of life and  
447 possibly to reveal significant aspects of this universally conserved pathway that may have gone  
448 unnoticed in other eukaryotic models.

449

## 450 **Materials and methods:**

### 451 **Plant Materials**

452 The genetic background for the *Arabidopsis thaliana* mutants and transgenic lines  
453 described in this study is the Col-0 accession. The following lines were described previously:  
454 *myb28-1 myb29-1* (70), *atg2-1* (18), *atg5-1* (58), *raptor1-1* (54, 55), *raptor1-2* (54), *raptor2-2* (54),  
455 *raptor2-1* (54, 55), and the *TORox* lines *G548*, *G166*, *S784*, and *S7817* (53). All genotypes were  
456 obtained and validated both genetically and phenotypically as homozygous for the correct allele.

457

### 458 **Plant growth media and *in vitro* root growth assays**

459 Seeds were vapour sterilized for 2-3 hours, by exposure to a solution of 100 mL household bleach  
460 (Klorin Original, Colgate-Palmolive A/S) mixed with 5 mL hydrochloric acid (12M), and ventilated  
461 for 30 min to one hour. After plating, on ½ strength Murashige and Skoog (MS) medium (2.2 g/l  
462 MS+vitamins) (Duchefa) with 1% (w/v) sucrose (Nordic Sugar), and 0.8% (w/v) micro agar  
463 (Duchefa), pH adjusted to 5.8), the seeds were stratified for two days in the dark at 4°C. For root  
464 length assays at normal light (115-130µE) *Arabidopsis* seedlings were grown vertically at 22°C day  
465 20°C night under a 16-h photoperiod and 80% humidity (long day). For meristem reactivation  
466 assays plants were grown as described in (12), except that in our conditions we needed to go to  
467 25µE to obtain meristem inhibition. Daily root lengths were manually marked (from day 3) with a  
468 permanent marker pen on the backside of the plate. After photography of 7-d-old seedlings the  
469 root growth was quantified using the ImageJ software(71). The least square means (lsmeans) for  
470 the genotypes in response to different treatments were calculated across experiments (in R, see  
471 statistics), and plotted in excel.

472

### 473 ***in vitro* root growth assays for the species (seed plating and growth conditions)**

474 To test 3OHP GSL perception in other plant orders, seeds were obtained as listed in table S1.  
 475 Except for *Solanum lycopersicum*, here *San Marzano* tomatoes were bought in a local supermarket  
 476 and the seeds were harvested, fermented and dried. All seeds were vapour sterilized for three  
 477 hours (as above). Before plating, and *Lotus japonicus MG20* (Lotus) were emerged in water and  
 478 kept at 4°C for 1-2 weeks. Seeds were plated on vertical ½MS plates as specified in table S1,  
 479 stratified for four days in the dark at 4°C before being transferred to a long day growth chamber).  
 480 Root growth was measured approximately every 24 hours (as described above).

481

482 **Table S1.**

Common name	Order	Family	Genus	Species	Subspecies	Supplier/Donor	Plate size (cm×cm)	Distance to top (cm)	Distance between seeds (cm)
Dill	Apiales	Apiaceae	Anethum	Graveolens	Mammut	Albertines A/S (Føtex)	12×12	6	2
Garden cress	Brassicales	Brassicaceae	Lepidium	Sativum	-	Albertines A/S (Føtex)	24×24	7	3
Rape seed	Brassicales	Brassicaceae	Brassica	Napus	-	a gift (see acknowledgements)	24×24	5	3
Rucola	Brassicales	Brassicaceae	Eruca	Sativa	Rouquette	Albertines A/S (Føtex)	12×12	3	2
Broccoli	Brassicales	Brassicaceae	Brassica	Oleraceae	Italica	Albertines A/S (Føtex)	24×24	7	4
Camelina	Brassicales	Brassicaceae	Camelina	Sativa	-	was a gift (see acknowledgements)	24×24	5	3
Lotus	Fabales	Fabaceae	Lotus	Japonicus	MG20	a gift (see acknowledgements)	12×12	6	2
Oregano	Lamiales	Lamiaceae	Origanum	vulgare	-	Albertines A/S (Føtex)	12×12	3	1
Tomato	Solanales	Solanaceae	Solanum	Lycopersicum	San marzano	Niels Møller Rasmussens Gartneri I/S (Kvickly)	24×24	7	2
Flax	Malpighiales	Linaceae	Linum	usitatissimum	-	Urtekram® International A/S, Midsona AB (Føtex)	24×24	7	3

483

484 **Sup. Table 1. Plant seeds used for *in vitro* root growth assays for the various plant species**

485 The, source, common name, order, family, genus, species, and subspecies seeds are listed for the used  
486 plant species. As well as the plate size (cm×cm), and plating distance used for the individual response  
487 assays.

488

489 **Yeast strain, media, and growth conditions**

490 The yeast strain, NMY51 with pOST1-Nubl and pDHB1-LargeT ((72, 73); DUALsystem Biotech), was  
491 grown in liquid YPD media (2% w/v bactopectone (Duchefa Biochemie), 1% w/v yeast extract  
492 (Becton, Dickinson and Company), 2% w/v glucose) with or without added GSLs, at 30°C and 150  
493 rpm shaking.

494

495 **Yeast growth assay**

496 On day one; a 5 ml overnight culture was started from cryostock. Day two; four new 4ml cultures  
497 were inoculated with 1 ml overnight culture, and grown overnight. On day three; an OD600 0.4  
498 and a 0.04 dilution was prepared from each of the four cultures. 500 µl of each of the four  
499 cultures, at both dilutions, were transferred to a 96-well culture plate containing 500 µl YPD liquid  
500 media with 3OHP GSL or Allyl GSL, to final OD600 0.2 and GSL concentrations of 50, 10, 5, 1 and 0  
501 µM. The yeast growth was measured at 0, 4, 6, 8, 24 and 48 hours. For each growth measurement  
502 100 µl culture was transferred to a 96-well Elisa-plate together with three wells of YPD liquid  
503 media for standardization. Growth was measured with a SpectraMAX 190 (Molecular Devices) and  
504 SoftMax® Pro 6.2.2 software. Growth rates and statistical analysis was calculated using the R  
505 software. The linear growth range was determined, and a linear regression using the lm() function  
506 in R was carried out to determine OD600 increase per hour (slope) and the yeast doubling time  
507 was calculated.

508

509 **Glucosinolate Analysis**

510 Glucosinolates were extracted from whole plant tissue of adult plants (for 3OHP GSL extraction),  
511 or from or 10-d-old seedlings (3OHP GSL uptake) (44, 74, 75), and desulfo-glucosinolates were  
512 analysed by LC-MS/TQ as desulfo-GSLs as described in (76).

513

514

515

516 **Statistics**

517 The R software with the R studio interface was used for statistical analysis (77, 78). Significance  
518 was tested using the Anova function (aov), lsmeans were obtained using the 'lsmeans' package  
519 (version 2.17) (79). The letter groupings (Tukey's HSD Test) were obtained using the 'agricolae'  
520 package (version 1.2-3) (80).

521

522 **Confocal Microscopy**

523 To examine the root tip zones, we used confocal laser-scanning microscopy of 4-d-old seedlings  
524 grown vertically with or without treatment (with 3OHP GSL and/or various inhibitors). Samples  
525 were mounted on microscopy slides in propidium iodide solution (40 $\mu$ M, Sigma) and incubated for  
526 15 minutes. Confocal laser scanning microscopy was carried out on a Leica SP5-X confocal  
527 microscope equipped with a HC PL FLUOTAR 10 DRY (0.3 numerical aperture, 10X magnification)  
528 or a HCX lambda blue PL APO 320 objective (0.7 numerical aperture, 20X magnification) for close-  
529 up pictures of the meristem. To visualize the cell walls of individual cells the propidium iodide stain  
530 was excited at 514 nm and emission was collected at 600 nm to 680 nm. To determine the size of  
531 the meristems the confocal pictures we manually inspected and the  
532 meristematic cells marked and counted (the meristem region is defined as in (1, 81)). To measure  
533 the distance from the root tip to the point of first root hair emergence we used ImageJ (71).

534

535 **Chemicals**

536 The AZD8055 (82), Torin2 (83), KU-63794 (84), and WYE-132 (85) were purchased from  
537 Selleckchem. PF-4708671 (86) and allyl/sinigrin were purchased from Sigma-Aldrich. 4MSB and  
538 3MSP GSLs were purchased at C2 Bioengineering. But-3-enyl GSL was purified from *Brassica rapa*  
539 seeds while 3OHP GSL was purified from the aerial parts of 4-5weeks old greenhouse-grown plants  
540 of the Arabidopsis accession Landsberg *erecta* (75, 76). The concentration of 3OHP and but-3-enyl  
541 GSL was determined by LC-MS/TQ as desulfo-GSLs. All inhibitors were dissolved in DMSO and  
542 stored as 10mM stocks at -20 °C. For allyl, 3MSP, and 4MSB ~100mM GSL stocks were made with  
543 H2O and the concentration of GSLs within these stocks was determined by LC-MS/TQ (see above).

544

545

546 **Funding:**

547 Funding for this work was provided by the Danish National Research Foundation (DNRF99) grant  
548 to DJK and MB, the NSF award IOS 13391205 and MCB 1330337 to DJK, and the USDA National  
549 Institute of Food and Agriculture, Hatch project number CA-D-PLS-7033-H to DJK.

550

551 **Acknowledgements:**

552 We thank the excellent technical assistance of the PLEN Greenhouse staff, and the DynaMo  
553 student helpers. We thank Dr. Svend Roesen Madsen for providing Camelina, and rape seeds, and  
554 Dr. Camilla Knudsen Baden for giving us lotus seeds.

555

556 **Conflict of Interest Statement:**

557 The authors declare that the research was conducted in the absence of any commercial or  
558 financial relationships that could be construed as a potential conflict of interest.

559

560 **References:**

- 561 1. Dolan L, Davies J. Cell expansion in roots. *Current opinion in plant biology*. 2004;7(1):33-9.  
562 2. Henriques R, Bogre L, Horvath B, Magyar Z. Balancing act: matching growth with  
563 environment by the TOR signalling pathway. *Journal of experimental botany*. 2014;65(10):2691-701.  
564 3. Smith AM, Stitt M. Coordination of carbon supply and plant growth. *Plant Cell Environ*.  
565 2007;30(9):1126-49.  
566 4. Rexin D, Meyer C, Robaglia C, Veit B. TOR signalling in plants. *Biochem J*. 2015;470(1):1-14.  
567 5. Galili G, Avin-Wittenberg T, Angelovici R, Fernie AR. The role of photosynthesis and amino  
568 acid metabolism in the energy status during seed development. *Front Plant Sci*. 2014;5:447.  
569 6. Sheen J. Master Regulators in Plant Glucose Signaling Networks. 2014;57(2):67-79.  
570 7. Lastdrager J, Hanson J, Smeekens S. Sugar signals and the control of plant growth and  
571 development. *Journal of experimental botany*. 2014;65(3):799-807.  
572 8. Baena-Gonzalez E. Energy signaling in the regulation of gene expression during stress. *Mol*  
573 *Plant*. 2010;3(2):300-13.  
574 9. Crozet P, Margalha L, Confraria A, Rodrigues A, Martinho C, Adamo M, et al. Mechanisms of  
575 regulation of SNF1/AMPK/SnRK1 protein kinases. *Front Plant Sci*. 2014;5.  
576 10. Baena-Gonzalez E, Rolland F, Thevelein JM, Sheen J. A central integrator of transcription  
577 networks in plant stress and energy signalling. *Nature*. 2007;448(7156):938-42.  
578 11. Sablowski R, Dornelas MC. Interplay between cell growth and cell cycle in plants. *Journal of*  
579 *experimental botany*. 2014;65(10):2703-14.  
580 12. Xiong Y, McCormack M, Li L, Hall Q, Xiang C, Sheen J. Glucose-TOR signalling reprograms the  
581 transcriptome and activates meristems. *Nature*. 2013;496(7444):181-6.  
582 13. Moreau M, Azzopardi M, Clement G, Dobrenel T, Marchive C, Renne C, et al. Mutations in  
583 the Arabidopsis homolog of LST8/GbetaL, a partner of the target of Rapamycin kinase, impair plant growth,  
584 flowering, and metabolic adaptation to long days. *Plant Cell*. 2012;24(2):463-81.

- 585 14. Menand B, Desnos T, Nussaume L, Berger F, Bouchez D, Meyer C, et al. Expression and  
586 disruption of the Arabidopsis TOR (target of rapamycin) gene. *Proc Natl Acad Sci U S A*. 2002;99(9):6422-7.
- 587 15. Deprost D, Truong HN, Robaglia C, Meyer C. An Arabidopsis homolog of RAPTOR/KOG1 is  
588 essential for early embryo development. *Biochem Bioph Res Co*. 2005;326(4):844-50.
- 589 16. Liu YM, Bassham DC. TOR Is a Negative Regulator of Autophagy in Arabidopsis thaliana. *Plos*  
590 *One*. 2010;5(7).
- 591 17. Shibutani ST, Yoshimori T. A current perspective of autophagosome biogenesis. *Cell research*.  
592 2014;24(1):58-68.
- 593 18. Inoue Y, Suzuki T, Hattori M, Yoshimoto K, Ohsumi Y, Moriyasu Y. AtATG genes, homologs of  
594 yeast autophagy genes, are involved in constitutive autophagy in Arabidopsis root tip cells. *Plant Cell*  
595 *Physiol*. 2006;47(12):1641-52.
- 596 19. Feng Y, He D, Yao Z, Klionsky DJ. The machinery of macroautophagy. *Cell research*.  
597 2014;24(1):24-41.
- 598 20. Le Bars R, Marion J, Le Borgne R, Satiat-Jeunemaitre B, Bianchi MW. ATG5 defines a  
599 phagophore domain connected to the endoplasmic reticulum during autophagosome formation in plants.  
600 *Nature communications*. 2014;5:4121.
- 601 21. Zhuang X, Chung KP, Jiang L. Origin of the Autophagosomal Membrane in Plants. *Front Plant*  
602 *Sci*. 2016;7:1655.
- 603 22. Züst T, Heichinger C, Grossniklaus U, Harrington R, Kliebenstein DJ, Turnbull LA. Natural  
604 enemies drive geographic variation in plant defenses. *Science*. 2012;338(6103):116-9.
- 605 23. Katz E, Nisani S, Yadav BS, Woldemariam MG, Shai B, Obolski U, et al. The glucosinolate  
606 breakdown product indole-3-carbinol acts as an auxin antagonist in roots of Arabidopsis thaliana. *Plant*  
607 *Journal*. 2015;82(4):547-55.
- 608 24. Bonawitz ND, Soltau WL, Blatchley MR, Powers BL, Hurlock AK, Seals LA, et al. REF4 and  
609 RFR1, Subunits of the Transcriptional Coregulatory Complex Mediator, Are Required for Phenylpropanoid  
610 Homeostasis in Arabidopsis. *Journal of Biological Chemistry*. 2012;287(8):5434-45.
- 611 25. Bonawitz ND, Kim JI, Tobimatsu Y, Ciesielski PN, Anderson NA, Ximenes E, et al. Disruption of  
612 Mediator rescues the stunted growth of a lignin-deficient Arabidopsis mutant. *Nature*. 2014;509(7500):376-  
613 +.
- 614 26. Kim JI, Ciesielski PN, Donohoe BS, Chapple C, Li X. Chemically induced conditional rescue of  
615 the reduced epidermal fluorescence8 mutant of Arabidopsis reveals rapid restoration of growth and  
616 selective turnover of secondary metabolite pools. *Plant Physiol*. 2014;164(2):584-95.
- 617 27. Francisco M, Joseph B, Caligagan H, Li BH, Corwin JA, Lin C, et al. Genome Wide Association  
618 Mapping in Arabidopsis thaliana Identifies Novel Genes Involved in Linking Allyl Glucosinolate to Altered  
619 Biomass and Defense. *Front Plant Sci*. 2016;7.
- 620 28. Francisco M, Joseph B, Caligagan H, Li BH, Corwin JA, Lin C, et al. The Defense Metabolite,  
621 Allyl Glucosinolate, Modulates Arabidopsis thaliana Biomass Dependent upon the Endogenous  
622 Glucosinolate Pathway. *Front Plant Sci*. 2016;7.
- 623 29. Sonderby IE, Geu-Flores F, Halkier BA. Biosynthesis of glucosinolates - gene discovery and  
624 beyond. *Trends in Plant Science*. 2010;15(5):283-90.
- 625 30. Lambrix V, Reichelt M, Mitchell-Olds T, Kliebenstein DJ, Gershenzon J. The Arabidopsis  
626 epithiospecifier protein promotes the hydrolysis of glucosinolates to nitriles and influences Trichoplusia ni  
627 herbivory. *Plant Cell*. 2001;13(12):2793-807.
- 628 31. Kliebenstein D, Pedersen D, Barker B, Mitchell-Olds T. Comparative analysis of quantitative  
629 trait loci controlling glucosinolates, myrosinase and insect resistance in Arabidopsis thaliana. *Genetics*.  
630 2002;161(1):325-32.
- 631 32. Clay NK, Adio AM, Denoux C, Jander G, Ausubel FM. Glucosinolate metabolites required for  
632 an Arabidopsis innate immune response. *Science*. 2009;323(5910):95-101.
- 633 33. Khokon MA, Jahan MS, Rahman T, Hossain MA, Muroyama D, Minami I, et al. Allyl  
634 isothiocyanate (AITC) induces stomatal closure in Arabidopsis. *Plant Cell Environ*. 2011;34(11):1900-6.

- 635 34. Bednarek P, Pislewska-Bednarek M, Svatos A, Schneider B, Doubsky J, Mansurova M, et al. A  
636 glucosinolate metabolism pathway in living plant cells mediates broad-spectrum antifungal defense.  
637 Science. 2009;323(5910):101-6.
- 638 35. Kerwin RE, Jimenez-Gomez JM, Fulop D, Harmer SL, Maloof JN, Kliebenstein DJ. Network  
639 quantitative trait loci mapping of circadian clock outputs identifies metabolic pathway-to-clock linkages in  
640 Arabidopsis. Plant Cell. 2011;23(2):471-85.
- 641 36. Jensen LM, Jepsen HSK, Halkier BA, Kliebenstein DJ, Burow M. Natural variation in cross-talk  
642 between glucosinolates and onset of flowering in Arabidopsis. Front Plant Sci. 2015;6.
- 643 37. Boller T, Felix G. A renaissance of elicitors: perception of microbe-associated molecular  
644 patterns and danger signals by pattern-recognition receptors. Annu Rev Plant Biol. 2009;60:379-406.
- 645 38. Chan EK, Rowe HC, Corwin JA, Joseph B, Kliebenstein DJ. Combining genome-wide  
646 association mapping and transcriptional networks to identify novel genes controlling glucosinolates in  
647 Arabidopsis thaliana. PLoS biology. 2011;9(8):e1001125.
- 648 39. Petersen BL, Chen S, Hansen CH, Olsen CE, Halkier BA. Composition and content of  
649 glucosinolates in developing Arabidopsis thaliana. Planta. 2002;214(4):562-71.
- 650 40. Brown PD, Tokuhiya JG, Reichelt M, Gershenzon J. Variation of glucosinolate accumulation  
651 among different organs and developmental stages of Arabidopsis thaliana. Phytochemistry.  
652 2003;62(3):471-81.
- 653 41. Fang J, Reichelt M, Hidalgo W, Agnolet S, Schneider B. Tissue-specific distribution of  
654 secondary metabolites in rapeseed (*Brassica napus* L.). PLoS One. 2012;7(10):e48006.
- 655 42. Kliebenstein DJ, D'Auria JC, Behere AS, Kim JH, Gunderson KL, Breen JN, et al.  
656 Characterization of seed-specific benzoyloxyglucosinolate mutations in Arabidopsis thaliana. Plant J.  
657 2007;51(6):1062-76.
- 658 43. Edger PP, Heide-Fischer HM, Bekaert M, Rota J, Gloeckner G, Platts AE, et al. The butterfly  
659 plant arms-race escalated by gene and genome duplications. P Natl Acad Sci USA. 2015;112(27):8362-6.
- 660 44. Kliebenstein DJ, Lambrix VM, Reichelt M, Gershenzon J, Mitchell-Olds T. Gene duplication in  
661 the diversification of secondary metabolism: Tandem 2-oxoglutarate-dependent dioxygenases control  
662 glucosinolate biosynthesis in Arabidopsis. Plant Cell. 2001;13(3):681-93.
- 663 45. Windsor AJ, Reichelt M, Figuth A, Svatos A, Kroymann J, Kliebenstein DJ, et al. Geographic  
664 and evolutionary diversification of glucosinolates among near relatives of Arabidopsis thaliana  
665 (Brassicaceae). Phytochemistry. 2005;66(11):1321-33.
- 666 46. Daxenbichler ME, Spencer GF, Schroeder WP. 3-Hydroxypropylglucosinolate, a New  
667 Glucosinolate in Seeds of *Erysimum-Hieracifolium* and *Malcolmia-Maritima*. Phytochemistry.  
668 1980;19(5):813-5.
- 669 47. Daxenbichler ME, Spencer GF, Carlson DG, Rose GB, Brinker AM, Powell RG. Glucosinolate  
670 Composition of Seeds from 297 Species of Wild Plants. Phytochemistry. 1991;30(8):2623-38.
- 671 48. Kliebenstein D.J. Chapter Three – Nonlinear Selection and a Blend of Convergent,  
672 Divergent and Parallel Evolution Shapes Natural Variation in Glucosinolates. Advances in Botanical  
673 Research. 2016;Volume 80:Pages 31–55.
- 674 49. Sabatini S, Heidstra R, Wildwater M, Scheres B. SCARECROW is involved in positioning the  
675 stem cell niche in the Arabidopsis root meristem. Genes & development. 2003;17(3):354-8.
- 676 50. Hao Y, Cui H. SHORT-ROOT regulates vascular patterning, but not apical meristematic activity  
677 in the Arabidopsis root through cytokinin homeostasis. Plant signaling & behavior. 2012;7(3):314-7.
- 678 51. Mikkelsen MD, Naur P, Halkier BA. Arabidopsis mutants in the C-S lyase of glucosinolate  
679 biosynthesis establish a critical role for indole-3-acetaldoxime in auxin homeostasis. Plant Journal.  
680 2004;37(5):770-7.
- 681 52. Boerjan W, Cervera MT, Delarue M, Beeckman T, Dewitte W, Bellini C, et al. Superroot, a  
682 Recessive Mutation in Arabidopsis, Confers Auxin Overproduction. Plant Cell. 1995;7(9):1405-19.
- 683 53. Deprost D, Yao L, Sormani R, Moreau M, Leterreux G, Nicolai M, et al. The Arabidopsis TOR  
684 kinase links plant growth, yield, stress resistance and mRNA translation. EMBO reports. 2007;8(9):864-70.

- 685 54. Deprost D, Truong HN, Robaglia C, Meyer C. An Arabidopsis homolog of RAPTOR/KOG1 is  
686 essential for early embryo development. *Biochem Biophys Res Commun*. 2005;326(4):844-50.
- 687 55. Anderson GH, Veit B, Hanson MR. The Arabidopsis AtRaptor genes are essential for post-  
688 embryonic plant growth. *BMC biology*. 2005;3:12.
- 689 56. Montane MH, Menand B. ATP-competitive mTOR kinase inhibitors delay plant growth by  
690 triggering early differentiation of meristematic cells but no developmental patterning change. *Journal of*  
691 *experimental botany*. 2013;64(14):4361-74.
- 692 57. Jia J, Zhu F, Ma XH, Cao ZWW, Li YXX, Chen YZ. Mechanisms of drug combinations:  
693 interaction and network perspectives. *Nat Rev Drug Discov*. 2009;8(2):111-28.
- 694 58. Thompson AR, Doelling JH, Suttangkakul A, Vierstra RD. Autophagic nutrient recycling in  
695 Arabidopsis directed by the ATG8 and ATG12 conjugation pathways. *Plant Physiology*. 2005;138(4):2097-  
696 110.
- 697 59. Velikkakath AK, Nishimura T, Oita E, Ishihara N, Mizushima N. Mammalian Atg2 proteins are  
698 essential for autophagosome formation and important for regulation of size and distribution of lipid  
699 droplets. *Mol Biol Cell*. 2012;23(5):896-909.
- 700 60. Ryabovol VV, Minibayeva FV. Molecular Mechanisms of Autophagy in Plants: Role of ATG8  
701 Proteins in Formation and Functioning of Autophagosomes. *Biochemistry Biokhimiia*. 2016;81(4):348-63.
- 702 61. Fujioka Y, Noda NN, Fujii K, Yoshimoto K, Ohsumi Y, Inagaki F. In vitro reconstitution of plant  
703 Atg8 and Atg12 conjugation systems essential for autophagy. *J Biol Chem*. 2008;283(4):1921-8.
- 704 62. Walczak M, Martens S. Dissecting the role of the Atg12-Atg5-Atg16 complex during  
705 autophagosome formation. *Autophagy*. 2013;9(3):424-5.
- 706 63. Kaufmann A, Beier V, Franquelim HG, Wollert T. Molecular mechanism of autophagic  
707 membrane-scaffold assembly and disassembly. *Cell*. 2014;156(3):469-81.
- 708 64. Li WW, Li J, Bao JK. Microautophagy: lesser-known self-eating. *Cellular and molecular life*  
709 *sciences : CMLS*. 2012;69(7):1125-36.
- 710 65. Barth C, Jander G. Arabidopsis myrosinases TGG1 and TGG2 have redundant function in  
711 glucosinolate breakdown and insect defense. *Plant Journal*. 2006;46(4):549-62.
- 712 66. Nakano RT, Pislewska-Bednarek M, Yamada K, Edger PP, Miyahara M, Kondo M, et al. PYK10  
713 myrosinase reveals a functional coordination between endoplasmic reticulum bodies and glucosinolates in  
714 Arabidopsis thaliana. *Plant J*. 2017;89(2):204-20.
- 715 67. Bones AM, Rossiter JT. The enzymic and chemically induced decomposition of glucosinolates.  
716 *Phytochemistry*. 2006;67(11):1053-67.
- 717 68. Park D, Jeong H, Lee MN, Koh A, Kwon O, Yang YR, et al. Resveratrol induces autophagy by  
718 directly inhibiting mTOR through ATP competition. *Sci Rep-Uk*. 2016;6.
- 719 69. Xie DX, Feys BF, James S, Nieto-Rostro M, Turner JG. COI1: An Arabidopsis gene required for  
720 jasmonate-regulated defense and fertility. *Science*. 1998;280(5366):1091-4.
- 721 70. Sonderby IE, Hansen BG, Bjarnholt N, Ticconi C, Halkier BA, Kliebenstein DJ. A systems  
722 biology approach identifies a R2R3 MYB gene subfamily with distinct and overlapping functions in  
723 regulation of aliphatic glucosinolates. *PLoS One*. 2007;2(12):e1322.
- 724 71. Schneider CA, Rasband WS, Eliceiri KW. NIH Image to ImageJ: 25 years of image analysis. *Nat*  
725 *Methods*. 2012;9(7):671-5.
- 726 72. Stagljar I, Korostensky C, Johnsson N, te Heesen S. A genetic system based on split-ubiquitin  
727 for the analysis of interactions between membrane proteins in vivo. *P Natl Acad Sci USA*. 1998;95(9):5187-  
728 92.
- 729 73. Mockli N, Deplazes A, Hassa PO, Zhang ZL, Peter M, Hottiger MO, et al. Yeast split-ubiquitin-  
730 based cytosolic screening system to detect interactions between transcriptionally active proteins.  
731 *Biotechniques*. 2007;42(6):725-30.
- 732 74. Kliebenstein DJ, Gershenzon J, Mitchell-Olds T. Comparative quantitative trait loci mapping  
733 of aliphatic, indolic and benzylic glucosinolate production in Arabidopsis thaliana leaves and seeds.  
734 *Genetics*. 2001;159(1):359-70.

- 735 75. Kliebenstein DJ, Kroymann J, Brown P, Figuth A, Pedersen D, Gershenzon J, et al. Genetic  
736 control of natural variation in Arabidopsis glucosinolate accumulation. *Plant Physiol.* 2001;126(2):811-25.
- 737 76. Crocoll C, Halkier BA, Burow M. Analysis and Quantification of Glucosinolates. *Current*  
738 *Protocols in Plant Biology*: John Wiley & Sons, Inc.; 2016.
- 739 77. Team RDC. R: a language and environment for statistical computing [http://www.R-](http://www.R-project.org/)  
740 [project.org/](http://www.R-project.org/).
- 741 78. Team R. RStudio: Integrated Development for R. <https://www.rstudio.com/2015>.
- 742 79. Lenth RV. Least-Squares Means: The R Package lsmeans. *J Stat Softw.* 2016;69(1):1-33.
- 743 80. Mendiburu Fd. *Agricolae: statistical procedures for agricultural research* [https://CRAN.R-](https://CRAN.R-project.org/package=agricolae2010)  
744 [project.org/package=agricolae2010](https://CRAN.R-project.org/package=agricolae2010).
- 745 81. Perilli S, Sabatini S. Analysis of root meristem size development. *Methods in molecular*  
746 *biology.* 2010;655:177-87.
- 747 82. Chresta CM, Davies BR, Hickson I, Harding T, Cosulich S, Critchlow SE, et al. AZD8055 Is a  
748 Potent, Selective, and Orally Bioavailable ATP-Competitive Mammalian Target of Rapamycin Kinase  
749 Inhibitor with In vitro and In vivo Antitumor Activity. *Cancer Res.* 2010;70(1):288-98.
- 750 83. Liu Q, Wang J, Kang SA, Thoreen CC, Hur W, Ahmed T, et al. Discovery of 9-(6-aminopyridin-  
751 3-yl)-1-(3-(trifluoromethyl)phenyl)benzo[h][1,6]naphthyridin-2(1H)-one (Torin2) as a potent, selective, and  
752 orally available mammalian target of rapamycin (mTOR) inhibitor for treatment of cancer. *Journal of*  
753 *medicinal chemistry.* 2011;54(5):1473-80.
- 754 84. Garcia-Martinez JM, Moran J, Clarke RG, Gray A, Cosulich SC, Chresta CM, et al. Ku-0063794  
755 is a specific inhibitor of the mammalian target of rapamycin (mTOR). *Biochem J.* 2009;421:29-42.
- 756 85. Yu K, Shi C, Toral-Barza L, Lucas J, Shor B, Kim JE, et al. Beyond Rapalog Therapy: Preclinical  
757 Pharmacology and Antitumor Activity of WYE-125132, an ATP-Competitive and Specific Inhibitor of  
758 mTORC1 and mTORC2. *Cancer Res.* 2010;70(2):621-31.
- 759 86. Pearce LR, Alton GR, Richter DT, Kath JC, Lingardo L, Chapman J, et al. Characterization of PF-  
760 4708671, a novel and highly specific inhibitor of p70 ribosomal S6 kinase (S6K1). *Biochem J.* 2010;431:245-  
761 55.
- 762